On the thermal decomposition of tert.-butyl hydroperoxide, its sensitivity to metals and its kinetics, studied by thermoanalytic methods.

Willms, T.; Kryk, H.; Oertel, J.; Hempel, C.; Hampel, U.; Knitt, F.;

Originally published:

February 2019

Thermochimica Acta 672(2019), 25-42

DOI: https://doi.org/10.1016/j.tca.2018.12.007

On the thermal decomposition of tert.-butyl hydroperoxide, its sensitivity to metals and its kinetics, studied by thermoanalytic methods.

Thomas Willms, Holger Kryk, Jana Oertel[1], Christian Hempel, Friedhelm Knitt and Uwe Hampel

Helmholtz-Zentrum Dresden - Rossendorf, Institute of Fluid Dynamics,
Bautzner Landstraße 400, 01328 Dresden, Germany

[1] Helmholtz-Zentrum Dresden - Rossendorf, Institute of Resource ecology,
Bautzner Landstraße 400, 01328 Dresden, Germany

t.willms@hzdr.de, h.kryk@hzdr.de, j.oertel@hzdr.de, f.knitt@hzdr.de, u.hampel@hzdr.de,

KEY WORDS

Tert.-butyl hydroperoxide, DSC, steel crucible, silcosteel®, gold, copper, TAM

Abstract:

The decomposition of hydroperoxides like tert.-butyl hydroperoxide (TBHP) due to reactions with reactor materials (wall reactions) is an important issue in the frame of industrial processes and the analysis of such compounds. Because of the high surface-volume ratio such heterogeneous reactions are also especially important in case of thermo-analytical measurements. Therefore, the decomposition of TBHP has been studied for the first time extensively by Differential Scanning Calorimetry (DSC) using differently coated high pressure stainless steel crucibles (uncoated, gilded, silicon coated) and a medium pressure crucible. Furthermore, the interaction of such materials with TBHP has been measured for the first time by Thermal Activity Monitoring (TAM). The material of the gilded copper blowout disc turned out to be the reason for the very different DSC curves published in literature and had the highest influence compared to the crucible body material and the pressure. To protect the sample against the blowout disc, an aluminium foil has been placed below the blowout disc. This changed the shape of the DSC curve completely. It became more similar to that obtained with the medium pressure crucible. Furthermore, the reaction mechanism, kinetics and chemical aspects of the decomposition of TBHP at different conditions have been discussed and kinetics has been investigated for the first time by an overall evaluation of the DSC curves and a model free kinetics approach. Using the linear relationship between the kinetic activation parameters the published values are compared to those of the present work.

1. Introduction

The properties of peroxides are largely determined by the peroxy group, which is very reactive since its homolysis occurs at rather low temperatures [1]. Tertiary hydroperoxides like tert.-butyl hydroperoxide (TBHP) are among the most stable hydroperoxides [2], although pure TBHP and solutions of TBHP with a mass fraction of more than 90 % in water have to be considered as explosive substances [3] which could react sensitive to heat, shock, friction or contamination and are capable of explosive decomposition at normal temperatures and pressures. Aqueous TBHP with a mass fraction of 70 % might also explode due to fast heating or in the presence of contaminants [4] (which has caused some accidents [5]), but it is quite stable under normal conditions at ambient temperatures until 38 °C [6] and therefore commercially available.

TBHP is industrially of big interest due to its importance as an initiator and oxidizer. It is applied as initiator e.g. for polymerizations of vinyl chloride, ethylene, and acrylates in petrochemical industry [7]. Furthermore, it is used in the frame of novel reactions developed in organic synthesis for selective oxidation reactions as it is

shown by the increasing number of articles using this oxidant (see [8], [9–11]). A variant of the well-known Sharpless epoxidation reaction [12] also has become important as the industrially used oxirane process [13] for the oxidation of propylene to propylene oxide. Dependent on reaction conditions, the thermal decomposition of TBHP leads to by-products such as di-tert.-butyl peroxide (DTBP), tert.-butanol (TBA), acetone, methanol etc. [14–17]. In industry, in the frame of its production from isobutane [13], in analytical devices [16] as well as in the lab [18], [19] its decomposition due to the presence of catalysing metal ions or metals needs to be prevented, since it causes product losses and accidents [20]. A study on the effect of various metals at 30 °C has been performed by Thermal Activity Monitoring (TAM) [21].

Most published DSC measurements concerning TBHP have been done in the frame of studies of the behaviour of TBHP towards additives e.g. metal ions [22], solvents like TBA, decane or nonane [23], mineral acids and bases [4], [24], the main subject being the investigation of thermal hazards with TBHP contaminated by other substances. DSC experiments with TBHP without additives have been performed mostly for comparison with such hazard testing experiments. Wang and Shu [23], Wang et al. [24], Wang [4], and Chou et al. [25] used disposable gilded high pressure (HP) steel crucibles with blowout discs of gold from Mettler-Toledo (MT). This type of crucible has often been used for such tests although the use of gilded vessels had already been put into question [26]. In 2017, Akiyoshi et al. [27], who investigated the influence of reactor materials for 41 substances, reported important differences between the experiments obtained with glass and steel vessels. They investigated the influence of different steels as vessel cap on the DSC curves and wrote that "it appears that the generated gas reacts with stainless steel" [27], without saying which gas it could be. Verhoeff [28] already found a substantially different Differential Thermal Analysis (DTA) curve using a glass vessel inside a stainless steel vessel for his measurements. DSC and DTA curves are not directly comparable, however, it is evident that the curve was much less complex than the DSC curves obtained by Chou et al. [25]. In view of the first order of the reaction expected from measurements at low concentrations [29], this shape of the DSC curves was not understandable. The results obtained in the present work with high pressure crucibles were in part similar to the results obtained with gold or steel crucibles in literature, mentioned before [4], [23–25]. However, the results of the DSC measurements in the present work with HP crucibles as well as those found in literature differed somehow from each other, despite very similar conditions[1]. Furthermore, using a medium pressure crucible, the DSC curve was much more similar to a first order reaction. In earlier investigations [2], [29–35] on the decomposition of TBHP, which have been performed at low concentrations (e.g. ≈ 0.02 mol/L), mostly a reaction order of one has been found [29], however, a higher reaction order has also been observed [36]. Liu et al. [20] investigated the kinetics of the decomposition of a higher concentration of TBHP and fixed the reaction order to one. Especially, in view of the complicated radical mechanism [29] (chapter 2), it is not obvious, that the reaction order is still one, since also a complete or partial bimolecular decomposition of hydroperoxides at high concentrations [37] has been discussed. Moreover, Tseng et al. [38] gave an nth order evaluation of some single measurements with n = 0.7. Furthermore, authors in previous works [25], [39] based their kinetic evaluations on single DSC curves, being rather complicated in shape (DSC and DTA respectively), which did not at all correspond to a first order signal.

So, an extensive study of the reaction has been performed and it has been investigated, theoretically and experimentally, more closely. Since no critical review of the cited literature data or detailed investigation

[1] Private message of PhD Annett Knorr (BAM): Big differences between similar measurements have also been observed at the BAM. The "Bundesanstalt für Materialforschung und –prüfung" (BAM) is the Federal Agency for Material Research and Testing

including chemical aspects of the DSC experiments had been done so far, the revealed problems identified in literature (see Table 5) will be discussed. Furthermore, reusable commercial HP stainless steel crucibles with gilded blowout discs of copper, as generally used for DSC experiments and also used at the BAM [3], had not been considered yet in former investigations, mostly disposable gilded crucibles [23–25] have been used. To study the reaction more in detail, in the present study we also investigated the dependence of the DSC curve on the crucible type, the mass and the heating rate. If – and only if – the DSC signal appeared to be a single signal - in contrast to the works of Liu et al. [20], Hara et al. [25] and Chou et al. [39] – the reaction has been evaluated kinetically.

It has to be said that DSC experiments are characterized by a low ratio of volume to surface area as also remarked by Verhoeff [28]. It is typical for reactions containing hydroperoxides that, in addition to the homogenous reactions, further heterogeneous reactions take place, which influence the product decomposition by interaction with the material of the wall [40]. Therefore, all results of DSC experiments with TBHP are influenced by a so-called wall effect and the reproducibility of the experiments has also been investigated, the problem being the suitability of the materials due to changes of the material surface. Wall reactions can add a considerable complexity to the reaction system.

Therefore, the DSC curves, which were mostly complicated and obviously not due to a first order reaction, also have been analysed by model free kinetics (MFK). MFK has already been applied to many other complex reactions [41–44] and for the first time additionally used in the present work to investigate the change of the activation energy of the decomposition of TBHP as a function of the conversion under various conditions.

In addition to the DSC experiments in the present work, micro calorimetry experiments with parts of different crucibles have been performed to know more about the influence of the material on the decomposition of TBHP. In the following, the mechanism of the decomposition and its kinetics is given, which will serve for the mathematic derivation of the reaction order and the explanation of the experimental observations.

2. Reaction mechanism and previous works

2.1. Elementary reactions

It is generally admitted that the initial reaction of the thermal decomposition of peroxides and hydroperoxides is the rupture of the peroxy bond (I) (eq.1) [30], [32].

$$(CH_3)_3CO-OH \xrightarrow{k_1} (CH_3)_3C-O^{\cdot} + OH^{\cdot} \qquad \text{(eq.1)}$$

However, a unimolecular decomposition of TBHP molecules according to (eq.1) as main reaction, implying clearly a first order reaction, is only assured in inert polar solvents, at very small concentrations and high temperatures [37], where the association is diminished. Compared to dialkyl peroxides, the unimolecular homolysis of hydroperoxides is less important than the so-called induced decomposition [30].

$$(CH_3)_3C-O^{\cdot} + (CH_3)_3C-OOH \xrightarrow{k_2} (CH_3)_3C-OH + (CH_3)_3C-OO^{\cdot} \qquad \text{(eq.2)}$$

The tert.-butoxyl radical formed by (eq.1) reacts with a reactive hydrogen of a TBHP molecule [32] (eq.2) to TBA. The even more reactive hydroxyl radical reacts in a similar way to (eq.2) and forms water instead of TBA. The peroxy radical formed according to (eq.2) has the longest half-life among all radicals participating in the reaction. Therefore, it exists sufficiently long to be detected by Electron spin resonance (ESR) [45], to collide and finally recombine. The resulting tetroxides (eq.3) have been established at very low temperatures (< -90 °C) [45], [46], [47], [48].

$$(CH_3)_3\,C-OO^{\cdot}\ +\ (CH_3)_3\,C-OO^{\cdot}\xrightarrow{k_3}(CH_3)_3C-OOOO-C(CH_3)_3 \qquad \text{(eq.3)}$$

This intermediate is important since due to the so-called cage effect the cleavage products are kept together which can change the composition of the product mixture. Depending on temperature, the decomposition of the tetroxide inside the solvent cage, gives oxygen and DTBP [17], [32] (eq.4), which can terminate the reaction, or tert.-butoxy radicals (eq.5) which initiate further reactions. Neglecting the tetroxide intermediate (eq.3), the formation of DTBP (eq.4) prevails at lower temperatures, low polarity and high viscosity

$$(CH_3)_3\,C-OO^{\cdot}\ +\ (CH_3)_3\,C-OO^{\cdot}\xrightarrow{k_4}(CH_3)_3C-OO-C(CH_3)_3+\ O_2 \qquad \text{(eq.4)}$$

whereas at higher temperatures in polar solutions the radical formation dominates (eq.5).

$$(CH_3)_3\,C-OO^{\cdot}\ +\ (CH_3)_3\,C-OO^{\cdot}\xrightarrow{k_5}2\,(CH_3)_3C-O^{\cdot}+O_2 \qquad \text{(eq.5)}$$

However, it seems that an external recombination of tert.-butoxy radicals, after dissociation outside the cage, to DTBP can be excluded [49]. This may also be related to the high reactivity of alkoxy radicals but might depend on their structure. At higher temperatures (> 100 °C), depending on solvent and concentration, the tert.-butoxy radical (eq.1) (eq.5) also cleaves. In this case, propanone [29] and methyl radicals are formed (eq.6) [17], [50].

$$(CH_3)_3\,C-O^{\cdot}\xrightarrow{k_6}(CH_3)_2C=O+\ CH_3^{\cdot} \qquad \text{(eq.6)}$$

Methyl radicals give numerous further reactions, which end in oxidation products (e.g. formaldehyde, formic acid, carbon monoxide and dioxide).

2.2. Thermo-analytical investigations

Although there are several thermo-analytical studies ([3], [4], [23–28], [51], [52]) including the decomposition of TBHP (aqueous solution with mass fraction of 70 % TBHP), only four thermo-kinetic studies, treating the decomposition of TBHP without further additives could be found. Chou et al. [25] evaluated a single DSC curve of the decomposition of TBHP in a gilded HP crucible with a blowout disc of gold. In view of the shape of the curve, the evaluation as a first order reaction seems to be doubtful. Hara et al. [39] obtained kinetic parameters and found a nearly linear first order plot for the decomposition of TBHP by thermogravimetric analysis (TGA). However, in view of the shape of the also measured DTA curve and its similarity to the curve of Chou et al. [25] (especially the kink and the linear part in the cooling branch of the DTA curve), the evaluation as a first order reaction appeared also questionable since it indicates the influence of some catalysing material for both measure-ments. Without an explanation of the shape of the DSC curves, the kinetics cannot be considered as fully estab-lished, and the activation energy of the homogeneous reaction might be influenced by that of further undefined reactions. Furthermore, a reaction order of one has not been explained yet, considering the complex reaction mechanism. Tseng et al. [38] performed measurements with a TA Q20 DSC at 1, 2, 4 and 6 K/min and evaluated each measurement using a nth order kinetics and an autocatalytic mechanism. The curves are very different from those given in other works but the used crucible is not specified. The nth order evaluations resulted in similar reaction orders n, pre-exponential factors k_0 and activation energy E_A (e.g. n ≈ 0.72 to 0.76, $\ln k_0 \approx$ 25.1 to 26.64, $E_A \approx$ 107.9 to 112.1) for each single non-isothermal DSC measurement, but error limits of the activation parameters have not been given. This shows that an overall reaction order n = 1 might not be true for this reaction mechanism. Quite different reaction orders have been determined for the isothermal measurements. The autocatalytic mechanism gave less coherent results concerning the reaction parameters. Although ASTM E698 is mentioned in the publication, a simultaneous evaluation of the experiments at all heating rates (overall evaluation) according to the ASTM E698 has not been performed.

The investigation of pure or highly concentrated TBHP at large quantities and high temperatures (>150 °C) [53] is not without danger. Therefore, it is difficult to perform experiments on the decomposition under such conditions [12]. Furthermore, due to the mixing gap of water and TBHP, the maximum concentration of a homogeneous aqueous solution below the upper solubility limit of about 69 to 70 % TBHP (depending on temperature [6]) is only about 15 %. For this reason, Wang and Shu [23] took a solution of TBHP with a mass fraction of 15 % for experiments using an adiabatic calorimeter VSP2. Using a mini-autoclave with a glass vessel, Knorr [3] determined a temperature and a pressure course but neither kinetic parameters nor heat quantities could be measured. Except for studies by DSC, there are very few works on the decomposition of highly concentrated TBHP. Beside DTA measurements, Verhoeff [28] performed thermal explosion tests with about 100 g TBHP (70% and 80 %) and gave the heat production as a function of temperature in a bigger vessel, without determining kinetic parameters. Liu et al. [20] performed a kinetic investigation of experiments with an adiabatic accelerating rate calorimeter (titanium bomb) using about 1.47 g TBHP[2]. They obtained a reaction heat of 1440 J/g, activation parameters have been determined assuming a reaction order n = 1, without giving error limits and without justification of the reaction order. The pseudo rate constant does not depend exactly linearly on the reciprocal temperature as claimed. The calculated constant activation energy contradicts the given diagram since the activation energy vs. temperature showed obviously a big linear increase with the temperature between 70 and 190 °C. A formula is missing, so the slope of the activation energy is not clear. Therefore, the model free kinetics will be investigated and the reaction order will be discussed before the kinetic evaluation (4.2.14).

3. Experimental

3.1. Materials

Several batches of aqueous TBHP solution with a specified mass fraction of about 70 % TBHP (LUPEROX™) have been purchased from Sigma Aldrich and stored in a refrigerator at 4 °C to 8 °C. They have not been purified further and contained traces of propanone, tert.-butanol and other products. Precise analytic data were not available. Since composition differences might influence the DSC curves, details on the TBHP batch, its age and TBHP content (obtained from the supplier upon request) and the result of our own iodometric analysis are given in Table 1. If not indicated otherwise, in the present work the product with the designation Batch 2012 was used.

Table 1: Details on the TBHP solutions 70 % in water (LUPEROX™ TBH70X, Sigma Aldrich).

Product	Delivery date	TBHP mass fraction %	
		supplier	Own analysis
Batch 2012	03.09.2012	69.0	68.0 ± 2.0
Batch 2015	06.07.2015	75.5	69.1 ± 0.6
Batch 2016	18.11.2016	71.4	68.2 ± 0.9

DSC Crucibles have been purchased from Mettler-Toledo. The crucible types and their properties are given in Table 2. Among those, reusable HP steel crucibles (no. 3) have been utilized to perform many experiments, which are also used at the BAM [3] for safety technical investigations.

[2] Probably ~70 % but they did neither give the concentration of the purchased TBHP nor that in the used sample.

Table 2: Crucible types (MT) used in the present work and their characteristics.

no.	Crucible type	Crucible body material	blowout disc material	Crucible cap material	total mass/ mg	Volume / µl	Pressure max./ MPa	remark
1	Medium pressure crucible (MP) ME-00026929	stainless steel (no. 1.4301)[1]	none	Stainless steel lid with Viton seal	312	120	2	Disposable
2	HP steel crucible ME-51140404	stainless steel (no. 1.4435)[1]	Blowout disc made of copper, coated with 2 µm gold, covering completely the crucible. (ME-51140403)	Stainless steel lid with a hole closed by the blowout disc	613	30	15	Reusable
3	HP steel crucible, gilded ME-51140405	stainless steel, gilded 5 µm						
4	HP steel crucible, ME-51140404 silicon coated	stainless steel, with amorphous silicon < 1 µm						Reusable, identical with no. 2, coated with Silcolloy™ 1000 by SILCOTEC

[1]material number of the material as given by supplier, further information on material numbers see [54].

The stainless steel of the HP steel crucibles has a high molybdenum content, is non-magnetisable and shows a reduced pitting corrosion. Silicon-coated HP crucibles with a layer of 0.5 to 1 µm Silicon have been obtained by coating HP crucibles with silicon via chemical vapour deposition (CVD) by SILCOTEC GmbH. All HP steel crucibles are sealed by gilded copper blowout discs. Other blowout discs than those used were not available. In some experiments, usual aluminium foil (thickness 13 µm) has been used to shield the sample against the blowout disc by placing it underneath the blowout disc before closing the crucible. The heat flow at base line level has been normalized to zero for the MP and HP crucible.

3.2. Methods

3.2.1. Thermal Activity Monitoring (TAM)

An isothermal calorimeter (Thermal Activity Monitor, TAM III, TA Instruments [55]) equipped with 12 single micro calorimeter channels was used to measure the heat flow continuously. Each calorimetric channel was con-structed in twin configuration with one side for the sample and the other side for a static reference. The twin configuration of sample and reference within a channel allows the heat-output power from the sample to be compared directly with the heat-output power from the inert reference. TAM III employs a thermostat tech-nology that controls the temperature within 0.1 mK over 24 h. The temperature can be set between 15 and 150 ° C. Typically, the background noise of the heat flow is less than 0.10 µW. A temperature of 30 °C was applied in this study, which also made a comparison possible with previously measured values [21]. Parts from the different DSC crucibles served as metal samples for the TAM measurements. Each sample has been prepared for the TAM measurement by placing the corresponding crucible part into a sample vial (TA sample vials, borosilicate glass 4 mL volume) and filling it with 2 mL TBHP. For each material sample a second sample vial has been prepared as a reproducibility test. Besides, two sample vials, filled with TBHP, without material samples, served as references. In a typical experiment, 12 glass vials have been prepared for measurement, closed and then measured 20 h by TAM. The presented heat flow is the smoothed curve of the mean value of the two reproducibility measurements. For the determination of the total heat, the heat flow from 1 h to 15 h reaction

time has been used. More details on the method and a justification of the procedure and reaction conditions have been published elsewhere [21].

3.2.2. DSC experiments

A differential scanning calorimeter DSC821e™ and appropriate crucibles (MT) given in Table 2 have been used to perform temperature programmed screening experiments. Temperature, tau-lag and heat flow have been calibrated. The sample has been filled in the selected crucible using an air displacement micropipette (Lab Solute, 0.5 µl to 10 µl). The sample mass for each DSC experiment has been realized with the balance AT261 DeltaRange (MT) with a precision of 0.01 mg (range up to 62 g). For all crucibles, the mass of the crucible (including sample) has been measured before and after the measurement to check for mass losses. STAR Software (MT) has been used to obtain the experimental data e.g. heat flow curves and specific heat production (J/g). For some kinetic evaluations, 3 to 4 measurements needed to be performed using different heating rates. Therefore, the samples have been heated from 20 °C to 260 °C (or 350 °C depending on sample mass and position of the last peak) at varying heating rates (1, 2, 4, 10 K/min).

3.2.3. Reaction kinetics

The STAR Software® (MT) has been used for the kinetic evaluation in conjunction with the modules “nth order kinetics” and “model free kinetics” (MFK). The submodules “nth order kinetics” and “ASTM E 698 Kinetics” from the module “nth order kinetics” as well as the submodule “Applied MFK” of the module “model free kinetics” have been used.

3.2.4. The module nth order

The options named “nth order kinetics” and ASTM E 698 permit the evaluation of a single measurement as a simple and of several experiments as a complex reaction, respectively [56]. They base on the reaction rate law and the Arrhenius equation, which describes the dependence of the reaction rate constant k on the temperature T with the pre-exponential factor k_0, the activation energy E_A and the universal gas constant R. In case of simple homogeneous nth order reactions, the reaction rate can be expressed as a function of the conversion α (eq. 7).

$$d\alpha/dt = k(T) * (1-\alpha)^n \text{ with } k(T) = k_0 * \exp\left(-\frac{E_A}{RT}\right) \quad \text{(eq. 7)}$$

In case of DSC measurements, the reaction rate and hence the conversion rate is determined on the basis of the measured heat flux. According to (eq. 8), the conversion course can be expressed by the ratio of the heat production measured from the base line during a certain reaction time t and the total heat production ΔH_{total} measured for the total reaction time.

$$\alpha(t) = \frac{\int_{t=0}^{t} \frac{dH}{dt} dt}{\Delta H_{total}} \quad \text{(eq. 8)}$$

The module “Applied kinetics” allows for simulating the DSC curve as well as calculating the conversion as a function of time based on the given formulas. ASTM E698 uses the Kissinger method [57], [58] to evaluate the activation parameters based on DSC measurements measured at several heating rates assuming a reaction order of $n = 1$. The reaction order n cannot be varied.

3.2.5. MFK

According to the name, no assumption of a specific kinetics or reaction model is necessary. In a more generalized form, the equation for the reaction rate of the homogeneous reaction (eq. 7) can be used for any kind of reaction, including complex heterogeneous reactions (eq. 9) with different conversion terms.

$$d\alpha/dt = k(T) * f(\alpha) \quad \text{(eq. 9)}$$

An important deficiency of the common model-fitting procedure is that there are several so-called kinetic triplets ($\ln(k_0)$, E_A, $f(\alpha)$), describing the same conversion curve, which are linearly correlated. This is called the compensation effect [59], [60], [61].

$$d\alpha/dt = d\alpha/dT * dT/dt \quad \text{(eq. 10)}$$

In the application of the common model-fitting procedure to complex reactions (e.g. heterogeneous reactions), the reaction model cannot be identified by the evaluation of a single non-isothermal DSC curve since both the conversion α and temperature T change simultaneously (eq. 10) and it is unknown how the total error of $d\alpha/dt$ is distributed on the expressions of $d\alpha/dT$ and dT/dt.

Therefore, a wrong reaction model results in an error of $f(\alpha)$, which is compensated by an error of the reaction constant $k(T)$ yielding the same $d\alpha/dt$ (eq. 9). Thus, under such circumstances, a clean separation of $f(\alpha)$ and $k(T)$ in expression $d\alpha/dt$ (eq. 9) is not possible. To solve this problem, Vyazovkin [62] developed the so-called isoconversional methods on the basis of the isoconversional principle. Using 4 to 5 DSC measurements with different heating rates, the process rate can be determined at the same conversion from different measurements. According to the requirements, only DSC measurements with non-crossing conversion curves have been used for evaluation. As a result of such method, the activation energy is obtained as a function of the conversion. This method already has been widely applied [41–44]. However, the activation energy calculated by isoconversional methods cannot be directly compared to the activation energy obtained with the nth order module.

4. Results and discussion

4.1. TAM Measurements

The heat production rates of TBHP in contact with the crucible bodies of all HP crucibles, the MP crucible as well as the cap of the MP crucible have been measured at 30 °C by TAM (Figure 1). It is not possible to distinguish the homogeneous reaction of TBHP from possible reactions with the surface of the glass vial (due to acidic groups (Si-O-H) or possible metal traces in the glass). However, as shown and discussed in the previous work [21], the blanc sample, measured in a vial without metal sample, including such reactions, gave a very low heat flow (Figure 2), which has been deduced from that obtained with the metal samples.

TAM curves of different blowout discs varied considerably and gave generally higher heat releases than the other crucible parts. Therefore, an example of a measured TAM curve of a blowout disc is given separately in Figure 2. For comparison, the TAM curves of the crucible body and a blank are also shown.

In a previous work, using a surface of about 200 mm^2, the heat releases of a variety of pure materials have already been measured by TAM [21]. Table 3 shows the total heats measured for the samples of the present work and those of the pure materials obtained in the previous work for comparison.

Table 3: Surfaces and total heats of the crucible parts. The values of the pure materials (calculated from measurements with 200 mm^2 material) used for comparison are taken from a previous work [21].

Crucible part	Heat measured for crucible part (present work)			comparable material	Heat measured for compared material
	Total heat / mJ	Total surface/ mm^2	Area-related heat / µJ/mm^2	-	Area-related heat/ µJ/mm^2
MP steel crucible body	334	252	1325	Stainless steel	635
MP steel crucible cap	292	237	1232		
HP Stainless steel crucible body	542	210	2585		
Gilded HP steel crucible body	646	210	3076	gold	2015
Silicon coated HP steel crucible body	141	210	674	silicon	110
Blowout disc	1540	86	17907	copper	21700

Taking into account the area of the samples, the results permit to estimate the reactivity of the corresponding samples. For the gilded steel crucible body, a higher area related heat (and heat flow) has been measured than for the HP steel crucible, which corresponds to previous findings [21]. The silicon coated HP steel crucible gave a much lower heat flow than the MP steel crucible, the gilded and the uncoated HP steel crucible (Table 3). This shows that the silicon layer was quite effective to protect TBHP against contact with steel. The heat flows measured for the parts of the MP crucible lay between the heat flows measured for the silicon coated and the other HP crucibles. As this has to be expected, the MP crucible body and its cap gave very similar results. Supposing an error of 5 % concerning the area and the integral heat measured for the MP crucible might explain the difference of the measured area-related heats of the body and the cap of the MP crucible (consisting of the same steel). However, the heat flow measured for the HP steel crucible is much higher than for the MP crucible. This cannot be understood on the basis of the material. As it can be seen from Table 4, the compositions of the stainless steels of the HP crucible and the MP crucible are similar [63].

Table 4: Composition of HP and MP crucible steels [63].

crucible	steel no.	C %	Si %	Mn	P %	S %	Cr %	Ni %	Mo %	iron %
HP crucible	1.4435	0.03	1.0	2.0	0.045	0.025	17.5	13.5	2.75	residue
MP crucible	1.4301	0.07	1.0	2.0	0.045	0.03	18.5	9.5	0	residue

The small difference of the nickel contents cannot be the principal reason for such a high difference of the total heats. The content of molybdenum is the biggest difference but its content is small and should not be very reactive although this has not been investigated yet. Apart from the material, the biggest difference is that the HP crucible has a thread for the cap whereas the MP crucible and its cap are just pressed together. Compared to the HP crucibles, the parts from the MP crucible are much smoother and also the surface could be determined more exactly. As rough materials give a higher heat flow, as shown by sandblasting [21], the heats obtained with such samples are hardly comparable. This might also be the principal reason for the observation, that the heats obtained with the crucible steels are much higher than those of the previous work [21], also obtained with smooth samples of stainless steel (no. 1.4401).

In a similar way, the steel coated with 5 µm gold of the gilded HP crucible gave an area-related heat of 3076

μJ/mm² for a period of time, which is bigger than that measured for pure gold (2015 μJ/mm²) [21] but in the same order of magnitude, considering the difference of roughness and the thread. The area-related heat obtained for the uncoated HP steel crucible (2581 μJ/mm²) was lower than that of the gilded one (3076 μJ/mm²) and much higher than that of the silicon coated HP crucible (671 μJ/mm²). However, although the high area-related heat measured for TBHP in contact with silicon coated steel (671 μJ/mm²) was much lower than that measured with stainless steel (2581 μJ/mm²), it still indicates a significantly higher reactivity of the silicon-coated steel than of a smooth silicon wafer (110 μJ/mm²) [21]. Measurement errors (surface area, heat flow) cannot explain such a 6-fold higher heat integral. The influence of the thread and a generally higher roughness of the surface could in part explain a higher reactivity, but this difference is unusually high. The oxidation states might be different but the formation of quartz on the surface should occur on the silicon wafer as well as on the coated crucible. It has to be suspected, that a combination of the oxidation state, the especially high surface, the porosity of the silicon coating and possibly coating defects of the surface resulted in a significantly higher integral reaction heat compared to pure silicon. In total, the results given before are in well agreement with the tendencies obtained by previous measurements with the corresponding metals [21].
The heat flow obtained with the blowout disc was especially high (Figure 2). In case of the HP crucible, the cap has not been measured since it does not get in touch with the sample during DSC experiments due to the blowout disc placed below it. Considering the smaller surface, the blowout disc resulted in a much higher heat flow signal than the body of the HP steel crucible. For the measured blowout disc, the two reproducibility measurements resulted in maximum heat flows of about 20 μW minimum and 40 μW yielding a mean value of the total heat of about 1.54 J. Due to the deviation of both reproducibility experiments, increasing during the last 10 hours, the total heat release may be affected by an error of about ±50 mJ. So the maximum heat release per surface obtained with the blowout disc was about 18.5 mJ/mm². This is near to the value measured for copper (22 mJ/mm²). The experiments showed that the chemical characteristics of the blowout discs were much closer to copper than to gold. Obviously, since the gold layer of 2 μm influenced only slightly the properties of the copper blowout disc, the layer thickness was not constant or contained copper by diffusion. Whereas the interdiffusion coefficient of gold into copper is small, that of copper into gold is high and causes – already at low temperatures as 350 °C – a significant diffusion [64] of copper in the gold surface. Therefore copper, which is very reactive towards TBHP [21], is present in the gold surface. This means that a contact of e.g. TBHP vapour with the blowout disc results in a copper-catalysed reaction influencing the heat flow curve.

4.2. DSC measurements

The DSC curves of the decomposition of TBHP already published [3], [4], [23–27], [51], [52]), measured mostly in gilded high pressure crucibles, showed a complicated shape. Suspecting an influence of the material of the crucible body, experiments with differently coated crucibles (uncoated stainless steel, gilded steel, silicon-coated steel) have been performed to identify the reason for the differences between the published DSC curves.

4.2.1. Influence of the HP crucible coating on the DSC curve (gilded blowout disc)

Since in literature commonly about 4 mg were used for the DSC experiments, the results of the DSC experiments with 4 mg at 4 K/min are represented first (Figure 3).

In all experiments with HP crucibles using a gilded copper blowout disc, independent of a crucible coating, the shape of the DSC curves was characterized by the presence of two major peaks, with a third smaller peak in the

middle and several distortions and peak shoulders. It was not what has to be expected for a first order reaction as this had been determined for small concentrations of TBHP [29] in the past.
The first peak with a maximum at about 120 °C was rather large, often with a small shoulder on the left in the bottom part and another one on the right of the summit of the peak, followed by a second small peak at about 175 ° C. At about 200 °C, between the first major peak and the second smaller peak, the heat flow is slightly below zero, since at such temperatures most reaction products should be in the gas phase after the liquid phase reaction.
Depending on the heating rate and mass, DSC curves always showed a sharp and high exothermic signal at higher temperatures of about 250 °C, followed by an endothermic peak at about 250 to 280 °C. Afterwards the base line returned to zero. The endothermic peak at the end might be interpreted as a hint that there was a mass loss. However, the maximum mass losses of the experiments were < 1 wt. %, lying in the order of the error of the balance.
Therefore, this endothermic peak should be due to an endothermic reaction or phase transition in the crucible. It could be explained by the formation of a liquid phase (due to the increasing pressure) from a reaction product (e.g. water) which is formed by the previous reaction at about 250 °C (probably a combustion) and which vaporises in the gas phase at higher temperatures.
DSC experiments obtained with a sample mass of about 2 mg TBHP, as used by Tseng et al. [38], at a heating rate of 4 K/min in HP steel crucibles with and without coating gave essentially the same result as a sample of 4 mg (Figure 4).

In case of 2 mg sample mass mostly the second peak was better separated from the first peak. In general, the onset temperatures of DSC curves obtained were lower than those with 4 mg but this was not always the case. Using a gilded HP crucible and a sample mass of 2 mg, the base line was rising slightly at the end. Due to these observations, the reproducibility (4.2.3) and mass dependence (4.2.5) have also been studied. In the following, the shape and the heights of the signals of the DSC curves obtained in the present work are compared to those in literature.

4.2.2. Comparison with literature

There were especially striking differences of the DSC curve of the decomposition of TBHP obtained by Wang and Shu [23] compared to those obtained in the present work. The maximum DSC signal measured by Wang and Shu [23] and Wang et al. [24] (given in W/g) was much higher (~4 times) than that of Chou et al. [25] (given in W/g), where the DSC curve of Wang and Shu [23] is just the base line corrected DSC curve of Wang et al.[24]. The value of the maximal height of the signal given by Wang et al. [24] was of the same order of magnitude as that of Knorr [3] which has been given in mW. Therefore, the DSC curve of Wang et al. [24] has been corrected by division of the DSC signal by the sample mass (≈4 mg) which gave a comparable result to the measurements of Chou et al. [25] and the present work[3]. Also the integration of the curve showed that the integral given by Wang et al. [24] would be wrong if the unity was W/g. Therefore, the DSC curves of Wang et al. [24]
(corrected), of Chou et al. [25] and of Knorr (unpublished, offered by the BAM), using comparable heating rates of 4 and 5 K/min, are given in Figure 5.

Considering the different volumes of the HP crucible body used in the present work (30 µl) and of that used by

[3] This signifies that the unit of the heat flow of the DSC curves, given by Wang and Shu [23] and Wang et al. [24], is wrong and must be mW instead of W/g. The unit given by Chou et al. [25] is also wrong (J/g) and should be W/g.

Chou et al. [25] (40 µl), using the same type of DSC apparatus, the DSC curve obtained in the present work (see Figure 3) has some similarity with that published by Chou et al. [25], also measured with a gilded crucible. The DSC curve of Knorr is not fully comparable since the heating rate is slightly higher (5 K/min) than the others. Like the DSC curve of the present work, the starting of the peak of the DSC curve of Knorr is shifted to lower temperatures which might be related to the smaller volume of the crucible (Table 5). However, in contrast to the results of the present work, the DSC curve measured by Wang et al. [24] showed a quite high first signal and a second smaller peak just behind the first, with a small shoulder at the bottom on the right of the first peak. The DSC curve of the decomposition of TBHP measured in an coated or uncoated HP steel crucible in the present work given in Figure 3 was more similar to the result found by Chou et al. [25]. The last peak of the curve measured by Chou et al. [25] was much higher and sharper and the first signal less high than that measured by Wang [4]. Similarly, in both works the base lines of the HP crucible curves decreased at the end into the negative region compared to that at low temperatures. An overview on the DSC measurements found in literature is given in Table 5.

Table 5: Overview of DSC experiments of the decomposition of aqueous 70 % TBHP found in literature.

origin	sample mass / mg	Crucible Volume / µL	Heating rate / K/min	Heat integral / J/g	Onset tempe-rature / °C	Peak tempe-rature / °C	DSC, crucible	Blowout disc
Knorr [3]	6	30	2.5	1312	100	153.0	DSC (PE), reuseable HP stainless steel crucible	Gilded copper blowout disc[a]
Knorr (unpub-lished)	4	30	5	1350	88	149.0		
Present work	4.13	30	4	1493	101.1	129.6	MT DSC 821e, reuseable HP steel crucible gilded 5µm	
Wang and Shu [23], Wang et al. [24]	4.4	40	4	1622	75	161.8	MT DSC 821, disposable HP steel crucible gilded 5 µm	ME-26732, blowout disc of gold[b]
Chou et al. [25]	4.2	40	4	2008	92	159.4	MT DSC 821e, disposable HP steel crucible gilded 5 µm	
Akiyoshi et al. [27]	10-20	68	2	1517 (ss)	89 (ss)	138 (ss)	EXSTAR DSC 7020, Stainless steel vessel (ss) and glass capillaries (gc)	none
				1464 (ss)	96 (ss)	135 (ss)		
				1775 (gc)	122 (gc)	201(gc)		
				1721 (gc)	124 (gc)	204 (gc)		
Tseng et al. [38]	2.5	unknown	1	883.6	110	135	TA Q20, no details	unknown
	2.3		2	999.0	117	143		
	2.7		4	746.2	123	149		
	2.3		6	858.5	128	155		

a: Knorr [3] (PE) Perkin Elmer b: given in article, according to MT only Au 700/ 535 with silver were available

For pure TBHP a theoretical value of 2500 J/g has been cited by Wang et al. [24] for the heat of decomposition of TBHP. Neglecting a possible endothermic signal of water, this would correspond to a maximum of 1750 J/g for an aqueous solution of 70 % TBHP. However as the underlying reaction is doubtful and the really occurring processes above 100 °C are complex (Chapter 2.1) and not exactly known, the value of the decomposition heat will not be further discussed.

The DSC curves of Tseng et al. [38] and Akiyoshi et al. [27] are not shown in Figure 5 since details of the

crucible type of Tseng et al. [38] are not given and the conditions of the DSC experiment of Akiyoshi et al. [27] were very different (see Table 5). However, despite such differences, the DSC curves of Akiyoshi obtained with a stainless steel vessel were in part similar to those of the present work concerning the number (3 main peaks) and shape of the peaks. Those obtained with glass capillaries showed a major peak at about 200 °C (Table 5) with a large shoulder on the left (peak temperature not given, estimated ~150 °C) but no peak at higher temperatures. The comparison of the results of other works with those of the present work showed that the DSC curves are similar concerning the shape but the number of peaks and their heights as well as the exact shape differ, even among the DSC curves obtained with the same crucible type (Wang and Shu [23], Chou et al. [25]). To understand these differences, the influence of further parameters will be studied in the following. First, the reproducibility of the DSC curves will be studied.

4.2.3. Reproducibility of measurements in high pressure crucibles

Due to the sensitivity of TBHP towards metals [21], changes of the surface of the crucible wall as well as any impurity of the crucible or of the TBHP sample could influence the DSC curve. Despite applying an extreme diligence in the sample and crucible preparation, using comparable sample masses and trying several cleaning procedures with organic solvents (e.g. pentane, ethanol) and drying, a high reproducibility of the DSC curves could not be obtained. They varied at least as much as curves given in literature (see section 4.2.2). Also the number of measurements measured with the same HP stainless steel crucible had an influence, especially after the second use. Figure 6 shows the results obtained with HP stainless steel crucibles.

The onset temperature of most DSC curves is similar, the shape of the first peak differing slightly. The position of the second peak differed most. In part the differences might be due to corrosion problems of the crucibles since small brownish coloured spots have been found on the wall of HP stainless steel crucibles. They increased with the number of uses and with the maximum temperature. The corrosion seems to be mainly due to the water content combined with the high oxygen content and temperature, since measurements with 75 % TBHP in DTBP gave no visible corrosion with HP stainless steel crucibles. Cleaning with a product for removing rust did not help to improve the reproducibility of the DSC curves.

As with gilded crucibles no significant corrosion had been expected, the reproducibility of DSC experiments with those crucibles has also been investigated. With each of three crucibles, two experiments have been done. Although two DSC curves obtained with a new crucible are more similar concerning the first part of the DSC curve, the third curve had a much different appearance. The second DSC measurement with each of the crucibles gave curves with a much lower onset temperature. The gilded crucible body walls were slightly tarnished. This confirms that gold, as used by Wang et al. [24] should also not be entirely inert in such experiments due to interactions of TBHP with gold which influence the following result. The DSC curves, obtained with gilded high pressure steel crucibles, depending on the number of uses are shown in Figure 7.

Measurements after more than two uses gave likewise varying DSC curves. Although the important first part of the DSC curves was mostly similar, especially the onset temperature was not always reproducible. The second sharp and high peak varied the most.

To change the material of the crucible body did not help to improve the reproducibility. Moreover, the curves were also complicated, but the DSC curves given in literature by Wang [51] differed significantly in shape from those shown in Figure 7. Therefore, we investigated the influence of the TBHP batch.

4.2.4. Study of the dependence of DSC curves in HP steel crucibles on the batch of TBHP

The DSC curves obtained with different HP crucibles and masses with the same batch (2012) (as shown before) compared to each other were more similar than compared to those obtained with other batches. It is remarkable that, in more than 50 experiments for the present work, a DSC curve with a similar shape like that found by Wang et al. [24] has never been observed with the TBHP batch 2012, mainly used in the present work. Therefore other batches have been used as well. As it can be seen in Table 1, the content of TBHP given for each batch by the supplier differed in part, as well as the exact contents of impurities. This might lead to a dependence of the DSC curve on the exact composition of the product including different amounts of TBHP, its decomposition products etc., varying with the batch. Therefore, the influence of the batch has also been investigated. An example for DSC curves with different batches is shown in Figure 8.

DSC curves vary considerably considering the number of peaks and their heights. As it can be seen in Figure 8, the batch 2015 gave a DSC curve, which is more similar to that of Wang and Shu [23] than that obtained generally with Batch 2012: The first peak is rather high, followed by a smaller peak. The DSC curve obtained with batch 2012 corresponds more to that of Chou et al. [25] (see Figure 5). The first peak is rather flat, the second one sharp and high, with a large shoulder in-between. Table 6 gives an overview of the characteristic data of the DSC curves given in Figure 8.

Table 6: Characteristics of the DSC curves obtained by the decomposition of 4 mg TBHP measured at 4 K/ min between 20 and 350 °C in HP crucibles.

Batch	Onset Temp. / °C	Temperature of peak maximum / °C	total integral / J/g
2012	100.79	117.20	1549.66
2015	118.73	140.00	1395.50
2016	103.70	128.53	1761.27

To verify the reproducibility of the DSC curves obtained with various batches, the experiments have been repeated. Figure 9 shows that a strict dependence of the DSC curve on the batch could not be found. Whereas, the DSC curves of the batches 2012 and 2015 were comparable, especially the DSC curve obtained for the batch 2016 was quite different. A quantitative evaluation of the DSC curves of Figure 9 is given in Table 7.

Not only the height of the signals changed but also the shape of the curve. In the same way the onset temperatures varied considerably and could not be attributed to a certain batch. Table 7 summarizes the main properties of the DSC curves given in Figure 9.

Table 7: Characteristics of the DSC curves obtained by the decomposition of 4 mg TBHP measured between 20 and 350 °C at a heating rate of 4 K/min in HP crucibles.

Batch	Onset Temp. / °C	Temperature of Peak maximum / °C	total Integral / J/g
2012	119.17	156.53	2407.87
2015	62.91	152.47	2118.65
2016	123.74	157.27	2065.63

Obviously using the same batch of TBHP gave rather different looking DSC curves and different characteristic temperatures and heat integrals per gram. These measurements show that DSC measurements of all batches of TBHP performed with HP crucibles gave strongly varying DSC curves which do neither have an appropriated (first order) shape nor a sufficient reproducibility to perform kinetic evaluations. The complicated shape of the DSC curves with additional peak shoulders, obtained with HP crucibles, is common to all batches and should have a common reason.

4.2.5. Influence of the mass

A general problem of HP crucible experiments to obtain the same DSC curve could be that the same pressure course must occur and a minimum final pressure must be present for the decomposition. A mass dependence of the DSC curve on the sample mass, especially at small sample masses, co hence be explained by the fact that the final pressure in the crucible depends on the crucible volume and, depending on temperature, a certain pressure must be present for the reaction to start. A dependence of the mass has also been indicated by Akiyoshi et al. [27]. To make this influence evident, DSC experiments have been measured using 6, 4, 1.5 and 0.9 mg TBHP (Figure 10).

A higher sample mass of 6 mg TBHP or more did not change neither the general appearance of the DSC curve nor its base line. With a sample of 2 mg (Figure 4) a slight increase of the baseline has been observed (Figure 4). Samples of less than 2 mg gave DSC curves with similar peaks but showed a strongly increasing base line (Figure 10). The onset temperatures might be different at lower sample masses but due to the different base lines they were difficult to compare.

A reason for the rising base line – equal to a rising heat flow - could not be clearly identified. An exothermic reaction of the reaction gases with the wall material, as suggested by Akiyoshi al. [27] (“it appears that the generated gas reacts with stainless steel”) can be excluded as explanation for the rising base line due to the gold coating. Perhaps the rising base line is related to the complete vaporisation of the sample whereas with higher masses in part a liquid phase and a nearly constant baseline are maintained until about 250 °C (as discussed for Figure 3). The most important result is that a lower mass did not change significantly the shape of the first peak to a first order signal. Since neither the mass nor the coating of the crucible body or the TBHP batch did change significantly the appearance of the DSC curve, also DSC experiments with MP crucibles have been performed.

4.2.6. DSC experiments at medium pressure

DSC experiments with MP crucibles, allowing a maximum pressure of 20 bar, also resulted in exothermic signals. However, although two signals also have been obtained, it was striking that the DSC curves were much simpler (Figure 11) than those obtained with HP crucibles. The DSC curve obtained for the TBHP decompositi-on consisted of one major exothermic signal followed by a small one at high temperatures. In contrast to the re-sults obtained with HP crucibles, using the three different batches (batch2012, batch2015, batch2016) for experi-ments with MP crucibles resulted in three DSC curves with nearly identical appearance (Figure 11).

In case of MP crucibles the batch had no influence on the DSC curve and the measurements correspond practically to a reproducibility measurement. A very good reproducibility has been obtained for the first signal, the onset temperature and the maximum temperature being very similar for all three measurements (Table 8).

Table 8: DSC Results obtained with 9.8 mg in MP crucibles at 4 K/min

Batch	Peak 1 Onset Temp. / °C	Peak 1 Temp. of Max. / °C	Peak 1 Heat Integral / J/g	Peak 2 Onset Temp. / °C	Peak 2 Temp. of Max. / °C	Peak 2 Heat Integral / J/g
2012	160.1	177.3	1577	245.0	252.7	71.9
2015	159.8	178.7	1599	255.6	260.53	54.5
2016	163.1	178.8	1586	247.3	253.3	38.1

Also the integral heats per g obtained in the MP crucible were practically identical within very small deviations. In contrast to HP crucibles, MP crucibles are generally not used for decomposition experiments of TBHP since the used Viton seals limit its use to temperatures below 230 °C. Furthermore, the seals are permeable to water above 200 °C[4] and withstand a maximum pressure of maximal 20 bar. Thus, they require samples with little or no gas evolution. Accordingly, due to the maximum temperature of 250 °C used in the experiments and the significant gas evolution, it was not possible to prevent mass losses at the end of the experiment. Mass losses were directly proportional to the duration of the experiment. Thus a constant mass flow at the end of the experiment has been obtained. The endothermic course at temperatures of about 210 °C observed for the MP crucible might be due to a change of the heat capacity caused by thermal decomposition of liquid products to gaseous products or already due to evaporation of the crucible content. Considering the problems of tightness above 230 °C, the reproducibility of the second peak at high temperatures of the measurements is necessarily lower. In a separate experiment with air, the VITON seal gave no exothermic signal up to 300 °C. If there is no exothermic reaction of the VITON seal due to the higher oxygen pressure, then the exothermic signal might be also due to the combustion reaction of a decomposition product. In this case, the signal would correspond to that obtained with the HP steel crucible and its height is only decreased due to the smaller oxygen pressure caused by the mass loss. The results with such MP crucibles gave decisive hints on the reason of the shape of the TBHP experiments with HP steel crucibles. If the differences in shape and the reproducibility problem only appear with HP crucibles, then the reason for such differences should be due to the material of the blowout disc, which is the main difference between such crucibles.

4.2.7. Influence of the HP crucible blowout disc

Due to the tightness problems with MP crucibles further experiments with HP crucibles have been performed protecting the sample against the blowout disc by a shielding material. The protection has been realised by an aluminium foil (13 µm) placed below the blowout disc. Figure 12 shows the DSC curve obtained with a HP steel crucible and a normal blowout disc, the DSC curve observed after shielding the blowout disc of the HP crucible by aluminium foil and that found with an MP crucible.

Using an aluminium foil shielded HP crucible, the shape of the first major peak changed significantly compared to a DSC experiment without sample protection. Compared to the MP crucible, the first peak was less high, more symmetric and the onset temperature shifted to a lower temperature. As with MP crucibles, a big major peak without “shoulders” and significant distortions has been found. This shows that the additional reactions, responsible for further heat signals causing the distortions and shoulders, are due to catalysis by the blowout disc, and that, as found by TAM, the copper-like behaviour of the blowout disc is mainly responsible for such reactions. However, it is not clear if the different curves are due to different surface properties of the blowout disc or a modification of the surface by attack of the TBHP. Placing pure copper foil below the blowout disc

[4] Personal message from Mettler-Toledo.

gave not the same problems. A closer look at the surface of some unused blowout discs showed significant differences of the surface. Hence, the varying DSC curves obtained with different TBHP batches in HP steel crucibles might be due to a combination of variations of the surface and the differing properties of the TBHP batch concerning the reaction with copper or gold. Due to the position of the blowout disc, the complicated shape of the DSC curves for experiments with unshielded blowout discs should mostly be due to gas phase reactions as this has also been indicated by Akiyoshi et al. [27] who investigated the influence of the steel cap on the DSC curves. They also concluded that the shape of the DSC curve is influenced to a greater extent by the steel type of the cap, due to gas phase reactions, than by the material of the crucible body. They wrote that "it appears that the generated gas reacts with stainless steel" [27]. Based on the reaction mechanism presented in chapter 2, this gas is oxygen. Concerning the pressure in the crucible, it has been found that using a sample mass of 16 mg the blowout disc of the crucible bursts at 300 °C by evolution of oxygen, thus creating a pressure of more than 150 bar. Supposing a decomposition according to (eq. 12) as unique reaction, in case of a sample mass of 4 mg TBHP, an oxygen concentration of more than 99.4 % is possible in the DSC crucible at the beginning. The corresponding partial pressure of oxygen would result in ≈25 bar oxygen. With 16 mg TBHP, taking into account the smaller free gas volume in the crucible, even a pressure of 200 bar would result, which explains bursting. However, off course pure oxygen will result in combustion reactions, which would explain the second peak at high temperatures as a consequence of the high oxygen content and pressure. This explanation is also supported by Verhoeff [28], stating that gas explosions may be initiated by hot metal walls of 175 to 225 ° C. It is striking that the onset temperature of the DSC curves obtained with the MP crucible is higher compared to that obtained with the HP crucible. In case of the MP crucible, the temperature of the peak maximum was shifted to 171 °C compared to a HP crucible with the aluminium foils shielded (156 °C) and the unshielded blowout disc. The MP crucible has only half of the mass of the HP crucible. However, the phi factor, being the ratio of the heat capacities of the sample and the reactor vessel, of the HP crucible, using the specific heat capacity of steel of 500 J/kg/K [65] cannot be the reason for the different onset temperatures. Based on the smaller crucible mass – and heat capacity - a smaller onset temperature would have to be expected. The ratio phi(MP crucible)/ phi(HP crucible) of both crucibles for the same sample size is always about 0.50 to 0.55. As the influence of the aluminium foil on the phi factor, ranging between phi = 23 for a mass of 6 mg and phi = 68 for a mass of 2 mg TBHP for a HP steel crucible, is negligible, no change of the onset temperature has to be expected for the high pressure crucibles with and without aluminium foil. However, the onset temperature of the DSC curve obtained with the HP steel crucible without aluminium foil is much smaller than that of the HP crucible with shielded blowout disc. Therefore, the reason for the different onset-temperatures should be the 4 fold higher volume of the MP steel crucible. As the total masses and the volumes of the HP crucibles with and without shielded blowout disc are practically the same, the different onset temperatures and peak shapes are only due to the aluminium foil and thus due to the catalytic effect of the blowout disc in case of the HP steel crucible. The higher onset temperature and higher temperature of the peak maximum is therefore due to the bigger void volume, since the pressure is reached later (at a higher temperature) in the MP crucible than in the HP crucible.

This is consistent with the volume dependency suggested for Figure 5, where the DSC curve of the present work (30 µl crucible volume) has a much lower onset temperature than those of Chou et al. [25] and Wang et al. [24] (40 µl crucible volume). A notable exothermic decomposition of TBHP not only needs a minimum temperature but also a certain pressure, which is typically created by the superheated vapours of the peroxide. Correspondingly, Verhoeff [28] recommends to avoid combinations of high pressures and\ or high temperatures

to avoid explosions. He also remarked that the thermal decomposition of TBHP should occur first mainly in the liquid phase, since a strong pressure increase did only take place at the end of the exothermic runaway reaction. Hara et al [39] observed by DTA and TGA measurements, that there is no exothermic peak at normal or low pressure and applied a pressure of about 50 bar. This is consistent with the differing onset temperatures obtained in the present work for different crucible types which can be explained in part by differing material characteristics of the crucible and in part by the dependence of the exothermic decomposition of peroxides on the pressure course which changes in case of a different crucible volume.

In case of both HP crucibles, a second quite strong peak appeared in the region 180 to 250 °C, whereas with the medium pressure crucible there is only a small second peak at a much higher temperature due to the lower pressure.

4.2.8. Reproducibility of experiments with steel crucibles and aluminium foil

Whereas the use of aluminium foil to protect the sample against the blowout disc simplified considerably the shape of the DSC curves resulting from the TBHP decomposition, the curves were still not well reproducible. Most important problems were the positioning and the stability of the aluminium foil as well as its influence on the tightness of the crucible. Aluminium pieces of several thicknesses (e.g. 13, 33, 50 µm) have been tried. Especially interesting was that, using the same silicon coated steel crucible and an aluminium shielding, the first measurement gave a single broad peak whereas later measurements gave a second peak just behind the first major peak. A separation of the two peaks seemed to take place. Those works could not be further deepened but they showed that two peaks are typical for high pressure crucibles.

4.2.9. Model free kinetics

To reveal differences between the measurements in differently coated high pressure crucibles (gilded, silicon coated or uncoated steel crucible), DSC experiments have been conducted at heating rates of 1, 2, 4 and 10 K/min (Figure 13(a)) and evaluated by MFK. The influence of the heating rate on the DSC curves obtained with the different HP crucibles was always similar. At increasing heating rate, all peaks appeared at higher temperatures and became higher. At lower heating rates the sample is longer in contact with the heated crucible compared to high heating rates. Therefore, the conversion reached at the same temperature is higher for a lower heating rate.

4.2.10. Example of an evaluation

It was considered that especially the first peak of the decomposition of TBHP should be affected the most by the crucible material used for the DSC experiment since only TBHP is sensitive to metals. Furthermore, the composition of the sample is only defined at the beginning of the DSC curve. At higher temperatures (>230 °C), TBHP should be completely destroyed and the occurring reactions are unknown. Therefore, the MFK evaluation has been performed only for the first peak of the results (Figure 13 (b, c)). The shape of the first peak and the conversion curves indicate a complex reaction.

4.2.11. Influence of the coating on the activation energy

The dependence of the activation energy on the conversion determined for an uncoated, gilded and a silicon coated crucible is given in Figure 14. Corresponding to the low heat flow by TAM and as expected due to previous TAM measurements [21], the silicon coated crucible gave the highest activation energy by MFK. In contrast to this, the analysis by MFK in general gave a higher activation energy for the gilded crucible than for

the uncoated steel crucible whereas by TAM the inverse tendency has been found. This might indicate a dependence of the temperature. Although the activation energies at low conversions are not exactly constant, the curves are mostly more or less oscillating around a constant value up to conversions of about 60 %. However, as shown before, the activation energy curves vary considerably at high conversions, approximately exponentially increasing above 60 % and afterwards strongly decreasing at the end of the first peak. A probable interpretation would be that, at the end of the DSC curves, other reactions become important than in the beginning. Possible reasons might be beginning consecutive reactions in the gas phase as a consequence of the higher pressure created in the crucible and the higher temperature.

In contrast to the 4 mg sample, the activation energy obtained in case of the 2 mg sample with the steel crucible increased nearly linearly, except for the range of 40 % and 60 % where it stayed practically constant (Figure 15). As observed with 4 mg TBHP, below a conversion of 45 % the activation energy by MFK determined from the DSC curves of 2 mg samples was lower for the gilded and the uncoated steel crucible than that obtained with the silicon-coated HP steel crucible. The activation energy obtained with a sample of 2 mg in a steel crucible stayed in the entire range below that found with the gilded crucible whereas that found for the silicon crucible merges with that of the gilded crucible in the conversion range of 45 to 75%. At higher conversions, in both cases 2 mg (50 %) and 4 mg (80 %), the activation energy courses found for the gilded and the silicon coated crucible converge and increase in part parallel to that of steel. It is striking that in case of 4 mg the activation energy course obtained with the gilded HP crucible crosses that obtained with the stainless steel crucible in the range of 60 to 70 % and, at higher conversions, the activation energy courses become much more complex than with a sample of 2 mg where the activation energy courses were more or less flat.

4.2.12. MFK evaluation of DSC curves obtained with MP and HP crucibles (with and without shielding by Al)

Although the general influence of the heating rate on the DSC curves is well known, the corresponding results are given to show that the results correspond well to what has to be expected despite the problems of tightness in case of the MP crucibles and the aluminium foil placed below the blowout disc. The Influence of the heating rate on the DSC curves (see Figure 16) obtained with MP crucibles has been investigated to perform an evaluation by MFK (results, see Figure 18).

Similarly, DSC curves of TBHP have been measured at different heating rates (Figure 17) using HP steel crucibles with an Al foil shielded blowout disc to determine the activation energy course (Figure 18).

In case of the DSC measurement at 10 K/min the second small peak is merged in part with the first peak. Although DTA curves and DSC curves cannot be directly compared, it is interesting that the shape of the DSC curves is very similar to the DTA curve observed by Verhoeff [28] with a closed steel vessel and an inner glass vessel. Using the experiments measured at different heating rates shown before, an analysis by MFK has been performed. Figure 18 shows that the activation energy (130 to 150 kJ/mol) obtained using HP crucibles with aluminium foil shielded copper blowout discs was significantly higher than that obtained with unshielded blowout discs (40 kJ/mol to 70 kJ/mol) and slightly higher than that obtained with MP crucibles.

Considering that the DSC curve should be mainly influenced by reactions in the gas phase (see discussion on the blowout disc 4.2.7), this could be expected since the aluminium used as shielding material against the blowout disc in the HP crucible should be less reactive than the stainless steel of the cap of the MP crucible (see Table 2 and Figure 1). As a constant activation energy of the reaction is necessary to describe the reaction by nth order kinetics, the decrease of the activation energy might explain the problem to simulate correctly the second part of the peak and result in the reaction orders n < 1 obtained by the simulation in case of uncoated stainless steel. Considerable variations of the activation energy were found at higher conversions. In case of the MP crucible, the decrease of the activation energy might be simply due to the evaporation of the substance. In case of aluminium foil for the protection of the sample there might be a problem of mechanical stability with the foil at very high pressures, leading probably to the observed oscillation of the activation energy. In total, between 20 and 80 % conversion the most constant activation energy has been found with the HP steel crucible using an Aluminium foil as shielding material.

The parameters obtained by the evaluation of DSC experiments using HP crucibles with aluminium shielded blowout discs as a reaction of nth order are given in Table 11.

4.2.13. Identification of reaction model

Tseng et al. [38] tried to evaluate their DSC measurements by an autocatalytic reaction measurement and by a nth order reaction, since in principle, due to the radical mechanism the reaction could be both a nth order reaction or an autocatalytic reaction. Accelerating, decelerating and sigmoidal reaction types can only be distinguished with difficulty by the shape of the DSC curve in case of dynamic DSC measurements, since $k_0(T)$ is not constant. Therefore, isothermal DSC measurements should be used to identify the reaction profile [66–68]. The temperature for the isothermal DSC experiment has been determined to 155 °C from the dynamic DSC measurement according to a test described by TA-Instruments [69] (see Figure 19). A nth order reaction typically has its maximum reaction rate [67] - and hence in case of isothermal experiments its maximum heat flow - at the beginning of the DSC curve [66][68].

Thus, according to [66][68] the shape of the isothermal DSC curve (see Figure 19) proves that the decomposition of TBHP is a nth order reaction and explains why the evaluation with an autocatalytic mechanism by Tseng et al. [38] gave no consistent results. In the following the reaction order will be discussed.

4.2.14. Reaction order of the decomposition of TBHP

On the basis of the unimolecular decomposition according to (eq.1), a simple first order reaction of the decomposition of TBHP might be taken for granted due to the works in the past [2], [29], [33]. However, only very low concentrations (< 0.1 mol/ L) have been investigated. Furthermore, depending on temperature and solvent, in non-polar solvents, dimers and trimers of TBHP have been detected [50]. Taking this into account, higher reaction orders have been explained by as a unimolecular decomposition of the dimer of TBHP (eq.11) [1] [37][70].

$$2\,(CH_3)_3CO-OH \xrightarrow{k_4} (CH_3)_3\,C-O\cdot + (CH_3)_3\,C-OO\cdot + H_2O \quad \text{(eq.11)}$$

However, the reaction orders n > 1 of TBHP found in such works have been explained by Benson [36] by chain reactions with the solvent. All experiments could be evaluated [36] on the basis of an activation energy i.e. disso-ciation energy of the peroxy bond of 175.83 kJ/mol. Higher decomposition rates of TBHP than expected have also been observed in other areas where TBHP is used. For example, in the frame of the styrene polymerization,

the measured high polymerisation rate cannot be explained by the slow unimolecular decomposition of TBHP therefore Benson [36] excluded the unimolecular homolysis reaction (eq.1) as a source of initiation. However, it is known [28] that due to induced decomposition, the apparent initiation rate of polymerisations is often higher than this has to be expected on the basis of the reaction rate of the homolytic unimolecular cleavage of TBHP. Hiatt and Irvin [29], investigating the first order reaction between toluene and TBHP in the temperature range of 170 to 190 °C ([TBHP] ≈ 0.02 mol/ L), observed a reaction rate of TBHP with toluene at 100 °C, which was not compatible with the activation parameters obtained at higher temperatures. The reaction rate at 100 °C was 20 times higher than expected on the basis of the activation parameters measured between 170 °C and 190 °C. They suspected an important wall effect, but could not really explain this phenomenon. Since, according to Hiatt and Irvin [29], the reaction was still of first order, the observation might also be related to the induced decomposition which should be favoured at higher association degrees due to lower temperature. Although the initial unimolecular decomposition reaction is without doubt of first order, a first order reaction for the overall reaction is not evident considering the complex mechanism given in chapter 2 and the high concentration of the starting product TBHP. Using the principle of Bodenstein's stationary-state method and the mechanism given by Milas and Irvin [32] with the reactions (eq.1), (eq.2) and (eq.5), it was not possible to derive a formula for the decomposition since no termination reaction for radicals was included. Also, the destiny of the remaining radicals from (eq.5) was unclear since no further reaction partner was available after consumption of all TBHP molecules. Therefore, the recombination of tert.-butylperoxy radicals to DTBP has been added (eq.4). For the reaction in general, this is probably a rough simplification since further reactions should occur, especially as a consequence of the formation of propanone and methyl radicals. However, other compounds have not been reported by Milas and Irvin [32] for the reaction at about 100 °C. In a similar way, further reactions have also been omitted by Benson [36], investigating the decomposition of TBHP in the presence of an alkane as solvent. As it seems that the higher decomposition rates observed by Benson [36] and by Hiatt and Irvin [29] have not been explained yet, an explanation for the case of lower temperatures will be given in the present work. According to Milas and Surgenor [2], the decomposition of TBHP at 97 °C gave practically only oxygen and a TBA mass fraction of 86 % after 30 h (eq. 12), which is usually cited as quantitative conversion to TBA [30].

$$2\,(CH_3)_3CO-OH \rightarrow 2\,(CH_3)_3COH + O_2 \qquad \text{(eq. 12)}$$

If their findings are correct, i.e. there was really no recombination product (also no propanone, methanal etc.), this can only be explained by a missing cage effect. In this case, the resulting tert.-butylperoxy radicals did probably collide but the polar environment favoured the dissociation to tert.-butoxy radicals and the formation of TBA. However, the destiny of the radicals formed at the end of the reactions when all TBHP is consumed is unclear. Then, reaction (eq.2) is not possible any more. Therefore, the plausibility of the reaction scheme given by Milas and Surgenor [2] is limited. Since it would be difficult to include all subsequent reactions in such a treatment, in a first approach, only reactions occurring at temperatures < 100 °C have been considered. Using the equations and the rate constants of the reactions given before (chapter 2), this hypothesis results in a first order reaction, as given in equation (eq.13) which should be valid for the conditions of the TAM measurements and at low temperatures of DSC experiments.

$$-\frac{d[TBHP]}{dt} = k_1 * \left(3 + \frac{2 * k_5}{k_4}\right) * [TBHP] \qquad \text{(eq.13)}$$

It can be seen from (eq.13) that the decomposition rate is proportional to the initial decomposition and depends on the relation of the formation of DTBP (eq.4) and of tert.-butoxy radicals (eq.5) i.e. the ratio k_5/k_4. In DSC

experiments, i.e. at higher temperatures, additional reactions like the formation of propanone might influence the measured order of the reaction. The statement of Benson [36] that due to induced decomposition the initiation is often faster than this has to be expected on the basis of the homolytic cleavage of TBHP [28] could therefore be shown mathematically. According to Benson [36], the activation energy of the decomposition of peroxides, which corresponds to the dissociation energy of the peroxy bond, should be in the order of magnitude of E_A = 176 kJ/mol. However, in case of DSC experiments, due to the high surface area ratio, the apparent activation energy is smaller due to wall reactions.

Reaction orders below one, e.g. 0.7 as found by Tseng et al. [38], had not been found yet for the decomposition of hydroperoxides. As the reactions occurring in the DSC experiment are not completely known, any reaction scheme would be speculative. Therefore, the derivation of a formula with a reaction order of n = 0.7 on the basis of a reaction scheme is difficult. However, a reaction order below one might indicate a formula of the type (eq.14) which is typical for processes where a second molecule of the same type influences the reaction [61] or catalytic processes prevail (e.g. wall effect).

$$-\frac{d[TBHP]}{} = \frac{k_1 * [TBHP]^1 + k_2 * [TBHP]^2}{k_3 + k_4 * [TBHP]^1} \qquad \text{(eq.14)}$$

The counter term could be explained by the partial decomposition of TBHP as a dimer (eq.11) [1][37][70]. As the reaction order of 0.7 has not been fully established yet, these findings have not been further studied.

4.2.15. Kinetic nth order evaluation

The shape of the DSC curves, indicating several reactions, has been neglected in the past by other researchers e.g. Wang and Shu [23], Wang et al. [24] and Chou et al. [25]. In the beginning, it has been tried to obtain a kinetic evaluation of the first peak of the DSC curves obtained by DSC experiments in usual HP crucibles with gilded copper blowout discs. Although the model free kinetics revealed constant activation energies for the first part of the DSC curve of small samples (2 mg), an evaluation of the first signal of single DSC curves by nth order kinetics did not result in reasonable activation parameters and reaction orders. Reaction orders differed between -3.25 and 4.99. Similarly, ln(k_0) gave unrealistic positive and even negative values. In the present work, a consistent evaluation of the measured DSC curves of TBHP decomposition obtained with uncoated or gilded HP steel crucibles as a reaction of first order or nth order was not possible, which is reasonable in view of the complex DSC curves. The kinetic evaluation of the results published by Chou et al. [25] and Hara et al. [39] is therefore questionable. In Table 8, a summary of the results found in literature is given. Other thermoanalytical techniques have been included due to the small number of thermoanalytic measurements available.

Table 9: Thermo-analytical results on the decomposition of aqueous 70 % TBHP solutions found in literature.

reference	Mass	Vol-ume	Heating rate /	ln(k_0)	E_A	n[a]	Exothermic heat integral	Onset temp.	Peak temp.	Measurement details
	mg	µL	K/min	k_0/ s^{-1}	kJ/mol	-	J/g	°C		
Hara et al. [39]	5	?	10	22.6[b]	105.8	1	-	78	131	DTA, 50 bar
Verhoeff [28]	11.9	?	2.5	-	87.3[c]	-[c]	1250.0	≈87[d]	163.6[e]	DTA, glass inside NiCr steel vessel
Chou et al. [25]	4.2	40	4	20.5	92.4	1[f]	2007.7	92	159.4	DSC
Tseng et al. [38]	2.5	?	1	25.1	107.9	0.7245	898.7	110	135	DSC
	2.3		2	25.4	108.6	0.7193	1022.0	117	143	
	2.7		4	26.6	112.1	0.7222	1006.9	123	149	

	2.3		6	25.4	108.3	0.7634	876.7	128	155	
Liu et al. [20]	1470	?	5	40.9	68.3	1[f]	1440.0	69.5	163.03[e]	Adiabatic accelerating rate calori-meter

[a:] n: Reaction order [b:] The original value $\ln(k_0/min^{-1}) = 26.7$ has been converted to $\ln(k_0/s^{-1})$; [c:] The equation $q = 1.1*10^{11}*\exp(-10{,}500/T)$ for the heat generation q (W/g) by DTA has been given. So $E_A = R*10{,}500$, n probably 1; [d:] estimated from diagram; [e:] maximum temperature; [f:] fixed

The result given by Liu et al. [20] has been obtained using a titanium bomb, which is reasonable for a compound like TBHP. Titanium has been shown to be little reactive towards TBHP, at least at 30 °C [21]. However, the determined activation energy is much lower than expected. Except for the present work, only Tseng et al. [38] provide kinetic single curve evaluations of DSC measurements at different heating rates, but did not perform an overall evaluation of such experiments according to ASTM E698. Furthermore, using a TA Q20 from TA Instruments, no parameters of the crucible (volume, material, etc.) had been given. According to TA-Instruments[5], only copper based blowout discs are available. It is therefore striking, that the DSC curves are less complex than this has to be expected from other measurements. An explanation or discussion of the reaction orders had not been given either.

4.2.16. Medium pressure crucibles

The DSC curves of TBHP decomposition obtained in MP crucibles have been evaluated kinetically separately as an nth order reaction (Table 10). An example is given in (Figure 19). The simulated curve corresponded well to the experimental curve. The evaluation of the DSC curves with the nth order module resulted in part in reaction orders about $n = 1$, in part, especially at small heating rates, in reaction orders of 0.6. The lower reaction order obtained at the low heating rate might be due to a higher influence of the wall material and is similar to that found by Tseng et al. [38]. However, an influence of the low heat flow on the evaluation or the mass loss during the experiment could be also the reason. Furthermore, all measurements in an MP crucible at different heating rates have been also evaluated together as a first order reaction by ASTM E698 (see line "overall" in Table 9). In this case the reaction order could not be fitted.

Table 10: Kinetic parameters obtained from DSC experiments (Figure 16) using 8.74 mg (± 6 %) TBHP in MP crucibles at different heating rates by single measurement evaluations and an overall evaluation by ASTM E698.

Heating rate / K/min	$\ln(k_0)$	E_A / kJ/mol	Reaction order n	Heat integral / J/g	Onset temperature / °C	Temperature of peak maximum / °C	Maximum heat flow / W/g
1	27.12± 0.09	123.12±0.32	0.60 ±0.004	1382.87	136.0	163.8	0.85
2	30.36± 0.27	134.30±0.96	0.64± 0.012	1533.98	142.8	170.3	2.03
4	34.57± 0.19	148.64±0.69	0.99± 0.008	1323.96	139.2	176.5	3.29
10	25.41± 0.11	115.56±0.41	0.92± 0.006	1452.66	136.0	189.7	7.07
overall	29.75	131.15	1.00	-	-	-	-

A typical example for the simulated and experimental heat flow curve of a single DSC experiment, in this case based on the kinetic evaluation of an experiment at 4 K/min, is shown in Figure 19. The difference between the experimental and the simulated curve (Figure 19) is most significant in the range of the cooling curve. A possible explanation is indicated by the higher experimental peak which could be explained by a lower heat capacity than

[5] Personal message of TA-Instruments

that assumed for the simulation. This might be explained by the change of the sample mass due to the decomposition of the TBHP and the subsequent escape of the emerging gases. In view of such changes, the result is satisfactory. However, the DSC curves as well as the results of the evaluation must be considered critically. In case of the MP crucible considerable mass losses occurred, which have been proportional to the duration of the DSC experiments. Such sample losses are due to the known partial or complete failure of the sealing at temperatures above 200 °C in conjunction with the higher pressure and should influence both, the base line and the kinetic evaluation. This problem will be discussed comparing the activation parameters with data from literature (Figure 20).

Despite this problem, the simulation curve showed clearly that, in contrast to most other published curves, the DSC curves obtained with a medium pressure crucible correspond well to a first order reaction.

4.2.17. HP crucibles with aluminium shielded blowout disc

To circumvent the problem of the mass loss, the kinetic evaluation has been repeated using data obtained in an HP crucible with aluminium shielded blowout disc. Although the activation parameters differ significantly, the resulting reaction rates are consistent, as this can be seen from the linear correlation between the values of $\ln(k_0)$ and the activation energy E_A [61] (compensation effect), shown in Figure 20.

Table 11: Kinetic parameters obtained from DSC experiments (see Figure 17) with 6.19 (± 6 %) mg TBHP at different heating rates in HP crucibles using aluminium foil as shielding material for the blowout discs by single measurement evaluations and by an overall evaluation.

Heating rate / K/min	$\ln(k_0/ s^{-1})$	E_A / kJ/mol	Reaction order n	Heat integral / J/g	Onset temperature / °C	Peak temperature / °C	Maximum power / W
1	19.02 ± 0.18	92.37 ± 0.60	0.94 ± 0.009	1363.86	125.8	155.8	0.62
2	34.42 ± 0.29	143.68 ± 1.00	1.05 ± 0.013	1086.30	125.5	156.6	1.37
4	16.92 ± 0.15	82.31 ± 0.51	0.99 ± 0.010	1638.19	108.0	165.8	2.43
10	38.13 ± 0.29	159.29 ± 1.04	1.08 ± 0.013	1515.80	121.5	176.0	3.92
overall	27.91	123.28	1.00				

Due to the different reaction orders, the obtained activation parameters cannot be compared to those of the evaluations of Tseng et al. [38]. The result of Hara et al. [39] (see Table 5) is consistent with the kinetic results obtained in this work lies on the correlation line. It seems that they used an aluminium vessel for their experiment. The result of Chou et al. [25] ($\ln(k_0) = 20.5$, $E_A = 92.38$ kJ/mol, $n = 1$) diverges significantly. The result of Chou et al. [25] seems to be influenced by the catalytic effect of copper. Although the protection of the sample against the copper blowout disc improved significantly the shape of the DSC curve, the TAM experiments (chapter 4.1) showed that aluminium is not totally inert either.

The kinetic values of Tseng et al. [38] lie very near to each other on a line parallel to and below the correlation line. They are not comparable to the other data due to the different reaction order (n ~ 0.7). The same is true for the kinetic results obtained by evaluation of single DSC curves of the MP crucible measurement at 1 K/min and 2 K/min which lie on the correlation line. The activation energy obtained with an MP crucible at 4 K/min is too low compared to the other measurements, with an activation energy difference to the correlation line near to that of Chou et al. [25].

In contrast to this, the activation parameters ($\ln(k_o) = 40.89$, $E_A = 68$ kJ/mol) measured by Liu et al. [47] with an adiabatic accelerating rate calorimeter lie not on the correlation line. As their conditions were very different

(sample mass > 1 g, adiabatic accelerating rate calorimeter instead of DSC) this is not surprising but shows that results are depending very much on reaction conditions. As also stated by Verhoeff [28], kinetic parameters measured in DSC crucibles cannot be transferred to bigger vessels, as done by Tseng et al. [38], due to the heterogeneous reactions of TBHP with metals and the very different metal surface - volume ratios.

5. Conclusions

Due to the few data concerning the decomposition of TBHP, an extensive investigation of the decomposition of aqueous TBHP by DSC measurements and TAM measurements has been performed. An important reproducibility problem of DSC experiments with TBHP has been identified in the present work and could be revealed also in literature. It has been shown that, in case of DSC experiments with TBHP, there is an important influence of the material of the crucible on the DSC curve causing huge variations between several measurements even using the same crucible type, TBHP batch and blowout disc. The DSC curves of Tseng et al. [38] seem to be different but the conditions used and the reproducibility of their curves are unknown. Since this problem has not been addressed in literature yet this problem has been extensively studied.

Furthermore, the shapes of the DSC curves obtained with MP crucibles and HP crucibles showed significant differences. MP crucibles gave a good first order signal whereas the generally used HP crucibles gave complicated DSC curves containing peaks with many shoulders and distortions. Whereas differences of the DSC curves obtained with differently coated HP steel crucibles (uncoated, gilded, silicon coated) could not be identified, the material of the blowout disc has an important influence on the DSC curve of the decomposition of TBHP, which can be reduced by shielding TBHP against the influence of the blowout disc (e.g. by using aluminium foil). The influence of the blowout disc material on the thermal decomposition behaviour could be explained by catalysis of the present reactions. The results indicate a reaction in the gas phase. The model free kinetics module included in the STAR software (MT) has been applied to show the influence of the crucible material on the decomposition of TBHP. The complicated shape of the DSC curve of the TBHP decomposition in a HP steel crucible with a usual blowout disc could be related to the copper content of the gilded blowout disc of such crucibles and the attack of such blowout discs by TBHP. The characteristics of such blowout discs were nearer to that of copper, as shown by TAM, than that of gold and reduced very much the activation energy. Moreover, it seems that copper diffuses easily in gold [64] the strong catalytic effect on the decomposition observed in the present work. The observed slight influence of the TBHP batch in case of HP crucibles on the DSC curve compared to MP crucibles might be due to the different compositions of the batches and the stronger catalytic effect of copper on the reactions of such varying components compared to steel.

In view of the complicated curve of the DSC experiments of TBHP in HP crucibles like those published in the past by Wang and Shu [23] and Chou et al. [25], most of the DSC curves already published could definitely not be evaluated as a first order reaction. In the present work the use of aluminium foil as shielding material for the blowout disc permitted to obtain curves justifying the evaluation by a first order kinetics. The evaluation of the DSC curves obtained with the MP steel crucible and with the aluminium shielded high pressure steel crucible resulted mostly in a first order reaction without previously fixing the reaction order.

Normally, due to the limited reproducibility of the DSC curves obtained with Aluminium as shielding material and the sample loss in the medium pressure crucibles, a kinetic evaluation of the DSC measurements can be only justified with difficulty. However, to get better results, a new type of blowout disc would be necessary to obtain reasonable DSC curves with HP crucibles since no blowout discs for HP crucibles could be found permitting a clean decomposition without strong catalytic effects. The needed blowout discs may be perhaps either made

from aluminium, titanium or a glass coated material. This should also improve the reproducibility of the DSC experiments. However, the production of such blowout discs is out of range for us and the good linear correlation of all data obtained in the present work with the data already published shows that the results are acceptable.

Using the Bodenstein's stationary-state method [71], it has been shown for the first time that the assumption of a first order kinetics even holds, if the mechanism comprises, not only the unimolecular scission of the peroxy bond but also further radical reactions like the formation of TBA and DTBP. The possibility of a lower reaction order, as found by Tseng et al. [38], could be confirmed. Furthermore, a qualitative explanation for such a reaction order has been given. In view of the significant influence of the material, further research in this field would be necessary to model the entire reaction system consisting of heterogeneous and homogeneous reactions.

6. Acknowledgements

The authors acknowledge the Helmholtz Association for support of the research within the frame of the Helmholtz Energy Alliance 'Energy Efficient Chemical Multiphase Processes' (HEA-E0004). Furthermore, we thank TA-Instruments and Mettler-Toledo for their general assistance, especially Mr. Ahrens from Mettler-Toledo, as well as the BAM and Mrs. PhD Knorr (BAM), respectively for the offered comparative measurement.

7. References

[1] N. A. Milas and S. A. Harris, "Studies in Organic Peroxides. V. t-Butyl Hydroperoxide.," *J. Am. Chem. Soc.*, vol. 60, no. 10, pp. 2434–2436, 1938.

[2] N. A. Milas and D. M. Surgenor, "Studies in organic Peroxides VIII- t-Butyl Hydroperoxide and Di-t-Butyl Peroxide.," *J. Am. Chem. Soc.*, vol. 68, no. 2, pp. 205–208, 1946.

[3] A. Knorr, "Anwendung der TRAS 410 auf die sicherheitstechnische Beurteilung einer Perestersynthese," Technische Universität Berlin, 2006.

[4] Y. W. Wang, "Thermally Incompatible Hazards of Aqueous tert-Butyl Hydroperoxide with Various Acids/Alkalis.," *Ind. Eng. Chem. Res.*, vol. 51, no. 23, pp. 7845–7852, 2012.

[5] T. C. Ho, Y. S. Duh, and J. R. Chen, "Case studies of incidents in runaway reactions and emergency relief.," *Process Saf. Prog.*, vol. 17, p. 259., 1998.

[6] lyondellbasell, "T-Hydro Tert-Butyl Hydroperoxide (TBHP) Product Safety Bulletin." lyondell, 2016.

[7] Akzonobel Functional Chemicals, "Initiators and Reactor Additifs for Thermoplastics.," *http:www.akzonobel-polymerchemicals.com*. 2012.

[8] E. . Korshin and M. D. Bachi, *Synthetic uses of peroxides in The chemistry of peroxides (II), Part 1, Patai Series: The chemistry of functional groups,*, vol. 2, no. 307. Wiley InterSciences, Jerusalem, Israel, 2006.

[9] S. K. Rout, S. Guin, K. K. Ghara, A. Banerjee, and B. Patel, "Copper catalyzed oxidative esterification of aldehydes with alkylbenzenes via cross dehydrogenative coupling.," *Org. Lett. 2012 and 14: 3982-5.*, 2012.

[10] X. F. Wu, J. L. Gong, and X. Qi, "A Powerful Combination: Recent Achievements on Using TBAI and TBHP as Oxidation System.," *Org. Biomol. Chem. 2014, DOI: 10.1039/C4OB00276H.*, 2014.

[11] P. Malik and D. Chakraborty, "Bismuth(III) Oxide Catalyzed Oxidation of Alcohols with tert-Butyl Hydroperoxide.," *Synthesis*, pp. 3736–3740, 2010.

[12] K. B. Sharpless and T. R. Verhoeven, "Metal-Catalyzed Highly Selective Oxygenations of Olefins and Acetylenes with TBHP.," *Aldri Chimica Acta*, vol. 12, no. 4, pp. 63–82, 1979.

[13] J.-J. Arpe, *Industrielle Organische Chemie, Bedeutende Vor- und Zwischenprodukte.*, 6. Auflage. Wiley-VCH Verlag GmbH & Co. KGaA; 6. vollständig überarbeitete Auflage, 2007.

[14] D. L. Allara, T. Mill, D. G. Hendry, and F. R. Mayo, "Low Temperature Gas Phase and Liquid Phase Oxidations of Isobutane.," *Adv. Chem. Ser.*, vol. 76, no. 29, pp. 40–57, 1968.

[15] U. Shah, S. M. Mahajani, M. M. Sharma, and T. Sridhar, "Effect of supercritical Conditions on the Oxidation of Isobutane.," *Chem. Eng. Sci.*, vol. 55, pp. 25–35, 2000.

[16] T. Willms, H. Kryk, and U. Hampel, "The gas chromatographic analysis of the reaction products of the partial isobutane oxidation as a two phase process.," *J. Chromatogr. A*, vol. 1458, pp. 126–135, 2016.

[17] D. E. Winkler and G. W. Hearne, "Liquid Phase Oxidation of Isobutane.," *Ind. Eng. Chem. Res.*, vol. 53, no. 8, pp. 655–658, 1961.

[18] T. Willms, H. Kryk, and U. Hampel, "Development of a modular microreactor for the partial hydrocarbon oxidation.," *Chem. Eng. Com*, no. 3, pp. 269–280, 2018.

[19] T. Willms, H. Kryk, M. Wiezorek, and U. Hampel, “Development of a Micro Reactor for the Isobutane Oxidation as a Multiphase Process.,” in *Proceedings of the 4th European Conference on Microfluidics-Microfluidics 2014-Limerick, Dec.10-12, 2014.*, 2014.
[20] H. Liu, L. Gu, Zhu, Liu Zhangrui Peng, and B. Zhou, “2012 International Symposium on Safety Science and Technology Evaluation on thermal hazard of ter-butyl hydroperoxide by using accelerating rate calorimeter,” *Procedia Engineering*, vol. 45, pp. 574–579, 2012.
[21] T. Willms, H. Kryk, J. Oertel, X. Lu, and U. Hampel, “Reactivity of t-butyl hydroperoxide and t-butyl peroxide towards reactor materials measured by a microcalorimetric method at 30°C.,” *J. Therm. Anal. Calorim.*, vol. 9, pp. 1–15, 2016.
[22] R. Hiatt, T. Mill, K. C. Irwin, and J. K. Castleman, “Homolytic Decomposition of Hydroperoxides. IV. Metal Catalyzed Decompositions.,” *J. Org. Chem.*, vol. 33, p. 1428, 1968.
[23] Y. W. Wang and C. M. Shu, “Calorimetric Thermal Hazards of tert-Butyl Hydroperoxide Solutions.,” *Ind. Eng. Chem. Res.*, vol. 49, no. 19, pp. 8959–8968, 2010.
[24] Y.-W. Wang, Y.-S. Duh, and C.-M. Shu, “Thermal Runaway Hazards of tert-butyl Hydroperoxide by Calorimetric Studies.,” *J. Therm.Anal.Calorimetry*, vol. 95, no. 2, pp. 553–557, 2009.
[25] H.-C. Chou, N.-C. Chen, S.-T. Hsu, C.-H. Wang, S.-H. Wu, I.-J. Wen, S.-J. Shen, and C.-M. Shu, “Thermal hazard evaluation of tert-butyl hydroperoxide mixed with four acids using calorimetric approaches,” *J Therm Anal Calorim*, vol. 117, pp. 851–855, 2014.
[26] M. Akiyoshi, K. Okada, S. Usuba, and T. Matsunaga, “Effects of various vessel materials on exothermic decomposition energy measurements.,” *Thermochimica Acta*, vol. 515, no. 1–2, pp. 6–12, 2011.
[27] M. Akiyoshi, K. Okada, S. Usuba, and T. Matsunaga, “Comparison between Glass and Stainless-Steel Vessels in Differential Scanning Calorimetry Estimation.,” *American Journal of Analytical Chemistry*, vol. 8, pp. 19–34, 2017.
[28] J. Verhoeff, “Explosion hazards of tertiary Butyl hydroperoxide (TBHP).,” *I. Chem. E. Symposium*, vol. 68, p. 3/T:1 – T:12, 1981.
[29] R. Hiatt and K. C. Irvin, “Homolytic Decompositions of Hydroperoxides V thermal Decompositions.,” *J. Org. Chem.*, vol. 33, pp. 1436–1441, 1968.
[30] R. Hiatt, *Hydroperoxides., Organic Peroxides (II)*. Wiley Inter-Sciences New York, London, Toronto., 1971, p. 87.
[31] R. Hiatt, “Organic Peroxides (II).,” D. Swern, Ed. Wiley Inter-Sciences New York, London, Toronto, 1971, p. 49.
[32] R. Hiatt, J. Clipsham, and T. Visser, “The Induced Decomposition of tert-Butyl Hydroperoxide.,” *Can. J. Chem.*, vol. 42, no. 12, pp. 2754–2757, 1964.
[33] R. Hiatt, T. Mill, K. C. Irwin, and J. K. Castleman, “Homolytic Decompositions of Hydroperoxides. II Radical induced Decompositions of t-Butylhydroperoxide.,” *J. Org. Chem.*, vol. 33, p. 1421, 1968.
[34] R. Hiatt, T. Mill, K. C. Irwin, and C. W. Gould, “Homolytic Decompositions of Hydroperoxides. III Radical-induced Decompositions of Primary and Secondary Hydroperoxides.,” *J. Org. Chem.*, vol. 33, p. 1430, 1968.
[35] R. Hiatt, T. Mill, and F. R. Mayo, “Homolytic Decompositions of Hydroperoxides. I. Summary and Implications for Autooxidation.,” *J. Org. Chem.*, vol. 33, p. 1416, 1968.
[36] S. W. Benson, “Kinetics of Pyrolysis of Alkyl Hydroperoxides and Their O-O Bond Dissociation Energies,” *J. Chem. Phys.*, vol. 40, no. 4, p. 1007, 1964.
[37] L. Bateman and H. Hughes, “The Thermal Decomposition of cycloHexenyl Hydroperoxide in Hydrocarbon Solvents.,” *J. Chem. Soc.*, pp. 4594–4601, 1952.
[38] J.-M. Tseng, T.-F. Hsieh, Y.-M. Chang, Y.-C. Yang, L.-Y. Chen, and C.-P. Lin, “Prediction of thermal hazard of liquid organic peroxides by non-isothermal and isothermal kinetic model of DSC tests,” *Therm Anal Calorim*, no. 109, pp. 1095–1103, 2012.
[39] Y. Hara, H. Nakamura, T. Jinnouchi, K. Matsuyama, and M. Shimizu, “The thermal decomposition of organic peroxides: the thermal decomposition of alkyl hydro peroxides and dialkyl peroxides.,” *Kogyo Kayaku*, vol. 52, p. 350, 1991.
[40] G. Mckay and J. A. Aga, “Product Formation In The Slow Oxidation Of Isobutane.,” *Combustion And Flame*, vol. 40, no. 2, pp. 221–224, 1981.
[41] S. Vyazovkin, “Model-free Kinetics. Staying Free of Multiplying Entities without necessity.,” *Journal of thermal analysis and calorimetry.*, vol. 83, no. 1, pp. 45–51, 2006.
[42] S. Vyazovkin, “Evaluation of activation energy of thermally stimulated solid-state reactions under arbitrary variation of temperature.,” *Journal of Computational Chemistry.*, vol. 18, no. 3, pp. 393–402, 1997.
[43] S. Vyazovkin, “Advanced isoconversional method.,” *J. Therm. Anal. Calorimetry.*, vol. 49, no. 3, pp. 1493–1499, 1997.
[44] S. Vyazovkin, “Modification of the integral isoconversional method to account for variation in the activation energy.,” *J. Comp. Chem.*, vol. 22, no. 2, pp. 178–183, 2001.

[45] E. Bennet, “Kinetic Electron Paramagnetic Resonance Study of the Reactions of t-Butylperoxyl Radicals in Aqueous Solution.,” *J. Chem. Soc. Faraday Trans.*, vol. 86, no. 19, pp. 3247–3252, 1990.
[46] G. Bartlett and P. Günther, “Oxygen Rich Intermediates in the Low Temperature Oxidation of t-Butyl and Cumyl Hydroperoxides.,” *J. Am. Chem. Soc.*, vol. 88, no. 14, pp. 3288–3294, 1966.
[47] J. E. Bennet, D. M. Brown, and B. Mile, “The Equilibrium between tertiary Alkyperoxy-radicals and tetroxide Molecules.,” *Chem. Commun.*, pp. 504–505, 1969.
[48] T. G. Traylor and F. D. Bartlett, “O18 Tracer Evidence of the Termination Mechanism in the Autooxidation of Cumene.,” *Tetrahedron Letters*, vol. 1, no. 45, pp. 30–36, 1960.
[49] A. Factor, C. A. Russell, and T. G. Taylor, “Bimolecular Combination Reactions of Oxy Radicals.,” *J. Am. Chem. Soc.*, vol. 87, p. 3692, 1965.
[50] C. Walling and L. Heaton, “Hydrogen Bonding and Complex Formation in Solutions of t-Butyl Hydroperoxide.,” *J. Am. Chem. Soc.*, vol. 87, no. 1, pp. 48–51, 1965.
[51] Q. Wang, W. J. Rogers, and M. S. Mannan, “Thermal risk assessment and rankings for reaction hazards in process safety,” *Journal Of Thermal Analysis And Calorimetry*, vol. 98, no. 1, pp. 225–233, 2009.
[52] Y. W. Wang, Y. S. Duh, C. M. Shu, and Y. S. Duh, “Characterization of the Self-Reactive Decomposition of tert-Butyl Hydroperoxide in Three Different Diluents.,” *Process Saf. Prog.*, vol. 26, no. 4, pp. 299–305, 2007.
[53] European Union Rapporteur [The Netherlands], “Risk Assessment Report, tertiary butylL Hydroperoxide,” European Union, 2010.
[54] Rime GmbH, “Material numbers.,” *https://www.rime.de/en/101/material-numbers/*, 2016.
[55] TA - Instruments, “TAM Isothermal microcalorimetry.,” *http://www.tainstruments.com/pdf/brochure/MicrocalorimetryBrochure.pdf*.
[56] Mettler-Toledo, “Kinetik n-ter Ordnung,” *https://de.mt.com/mt_ext_files/Editorial/Generic/4/stare_kinetics_nthorder_datasheet_0x0002494700025 5120005c9cb_files/51724804.pdf (accessed 28.11.2018)*.
[57] H. E. Kissinger, “Reaction Kinetics in Differential Thermal Analysis,” *Analytical Chemistry*, vol. 1702, no. 29, pp. 1702–1706, 1957.
[58] S. Vyazovkin, K. Chrissafis, L. D. Lorenzo, N. Koga, M. Pijolate, N. Sbirrazzuoli, and J. J. Suñol, “ICTAC Kinetics Committee recommendations for collecting experimental thermal analysis data for kinetic computations,” *Thermochim. Acta*, vol. 590, pp. 1–23, 2014.
[59] R. Brown, “The Linear Enthalpy-Entropy Effect.,” *J. Org. Chem.*, vol. 27, no. 9, pp. 3015–3026, 1962.
[60] H. L. Anderson, A. Kemmler, and R. Strey, “Erfahrungen mit vier Softwarepaketen für kinetische Auswertungen in der thermischen Analyse,” *Journal of Thermal Analysis*, vol. 47, no. 2, pp. 543–557, 1996.
[61] T. Willms, “Kalorimetrische Untersuchungen zur Kinetik der Alkoholyse von Acylchloriden.,” Universität Greifswald, Germany, Shaker Verlag, 1999.
[62] S. Vyazovkin, *Isoconversional Kinetics of Thermally Stimulated Processes*. Springer International Publishing, 2015.
[63] tetec thermo-technik Müller GmbH & Co.KG, “Vergleichstabelle von Stahlsorten.,” *www.tetec-mueller.de/Dokumente/Pdf/Common/d/Material1_d.pdf*, 2016.
[64] R. Ravi and A. Paul, “Diffusion mechanism in the gold-copper system.,” *J. Mater Sci. Mater. Electron*, no. 23, pp. 2152–2156, 2012.
[65] D. Edelstahlwerke, “Acidur 4301 Werkstoffdatenblatt X5CrNi18-10.” Deutsche Edelstahlwerke, Aug-2017.
[66] R. Blaine, “A Review of DSC Kinetics Methods,” *http://www.tainstruments.com/pdf/literature/TA073.pdf (accessed at 25.11.2018)*.
[67] S. Vyazovkin, A. K. Burnhamb, J. M. Criadoc, L. A. Pérez-Maquedac, C. Popescud, and N. Sbirrazzuolie, “ICTAC Kinetics Committee recommendations for performing kinetic computations on thermal analysis data.,” *Thermochim. Acta*, vol. 590, pp. 1–23, 2011.
[68] *ASTM E2070 - 03, Standard Test Method for Kinetic Parameters by Differential Scanning Calorimetry Using Isothermal Methods*. ASTM International, West Conshohocken, PA, 2003.
[69] R. Blaine, “Practical Aspects of Kinetics - Determination by Thermal Analysis.,” *https://www.tainstruments.com/practical-aspects-of-kinetics-determination-by-thermal-analysis (accessed 25.11.2018)*, 2018.
[70] K. Ueberreiter and W. Rabel, “Die Beschleunigung des Hydroperoxydzerfalls durch Wasserstoffbrückenbildner in Lösung und bei der Polymerisation.,” *Makromol. Chemie*, vol. 68, pp. 12–23, 1963.
[71] S. Matsumoto, “Considerations of the Applicability of Bodenstein’s Stationary State Method to a certain problem of chemical kinetics.,” *Tech. Bull. Fac. Agr. Kagawa Univ.*, vol. 11, no. 29, pp. 275–280, 1959.

Titles of Figures

Figure 20: Simulated and measured DSC curve of the decomposition of 6 mg TBHP in a MP crucible between 25 and 225 °C at a heating rate of 4 K/min.

Figure 21: Linear relationship between the pre-exponential factor $\ln(k_0)$ and the activation energy E_A of the decomposition reaction of TBHP (reaction order n) obtained in literature and the present work (using HP crucibles (blowout disc shielded with Al) and MP crucibles) by nth order evaluation and ASTM E698 overall evaluation (n=1).

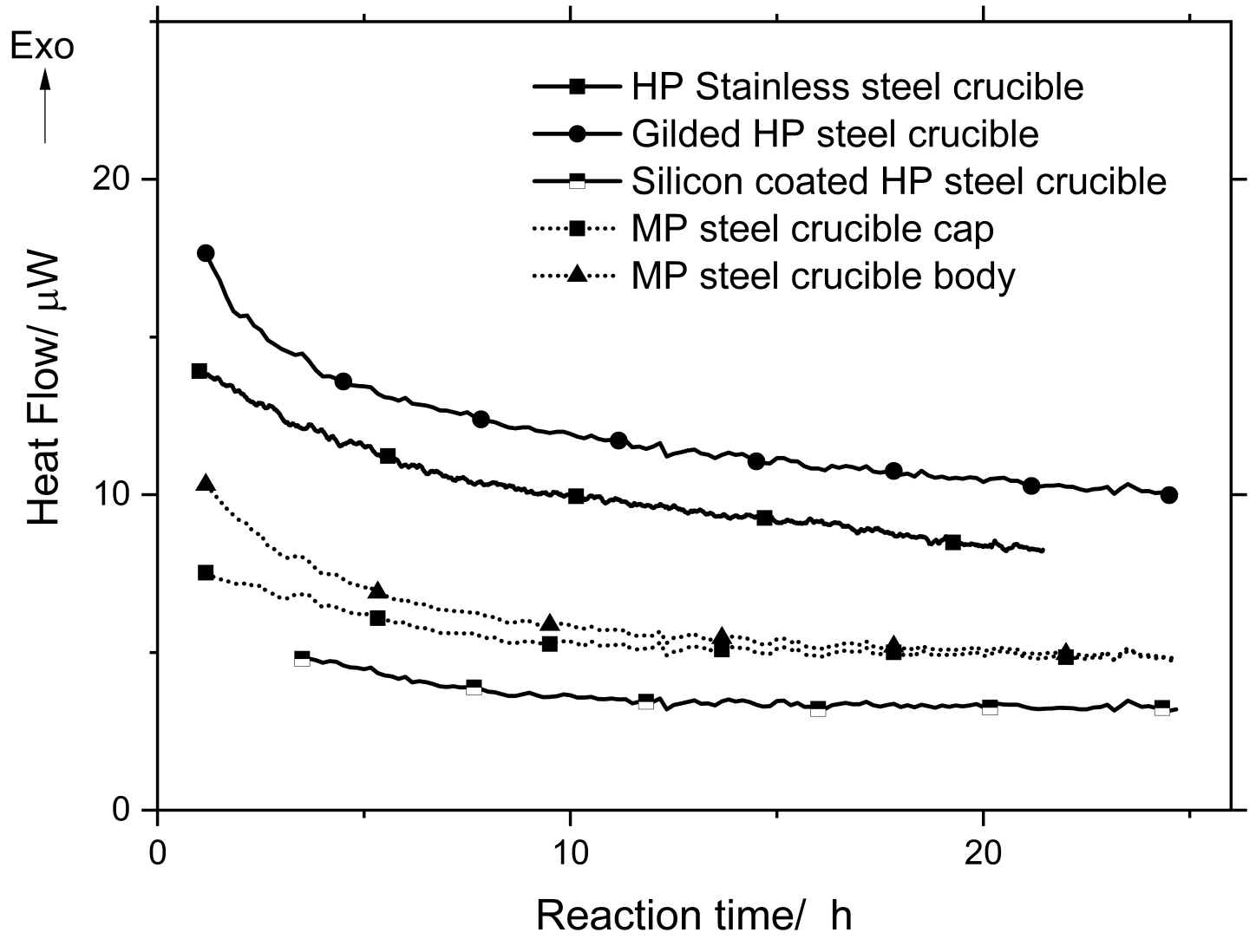
Exo
Heat Flow/ μW
20
10
0
0
10
20
Reaction time/ h
HP Stainless steel crucible
Gilded HP steel crucible
Silicon coated HP steel crucible
MP steel crucible cap
MP steel crucible body

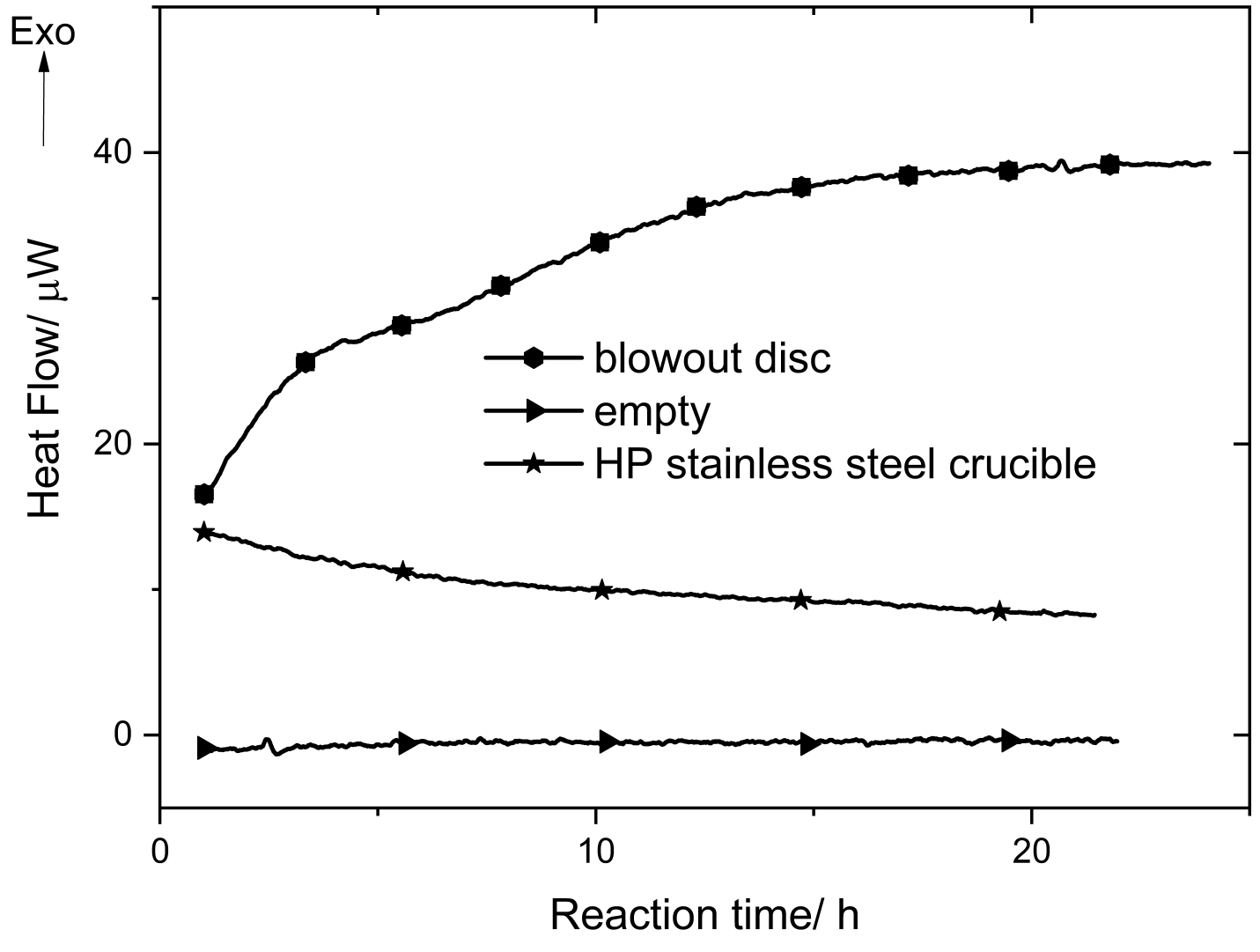
Exo
Heat Flow/ μW
40
20
0
0
10
20
Reaction time/ h
blowout disc
empty
HP stainless steel crucible

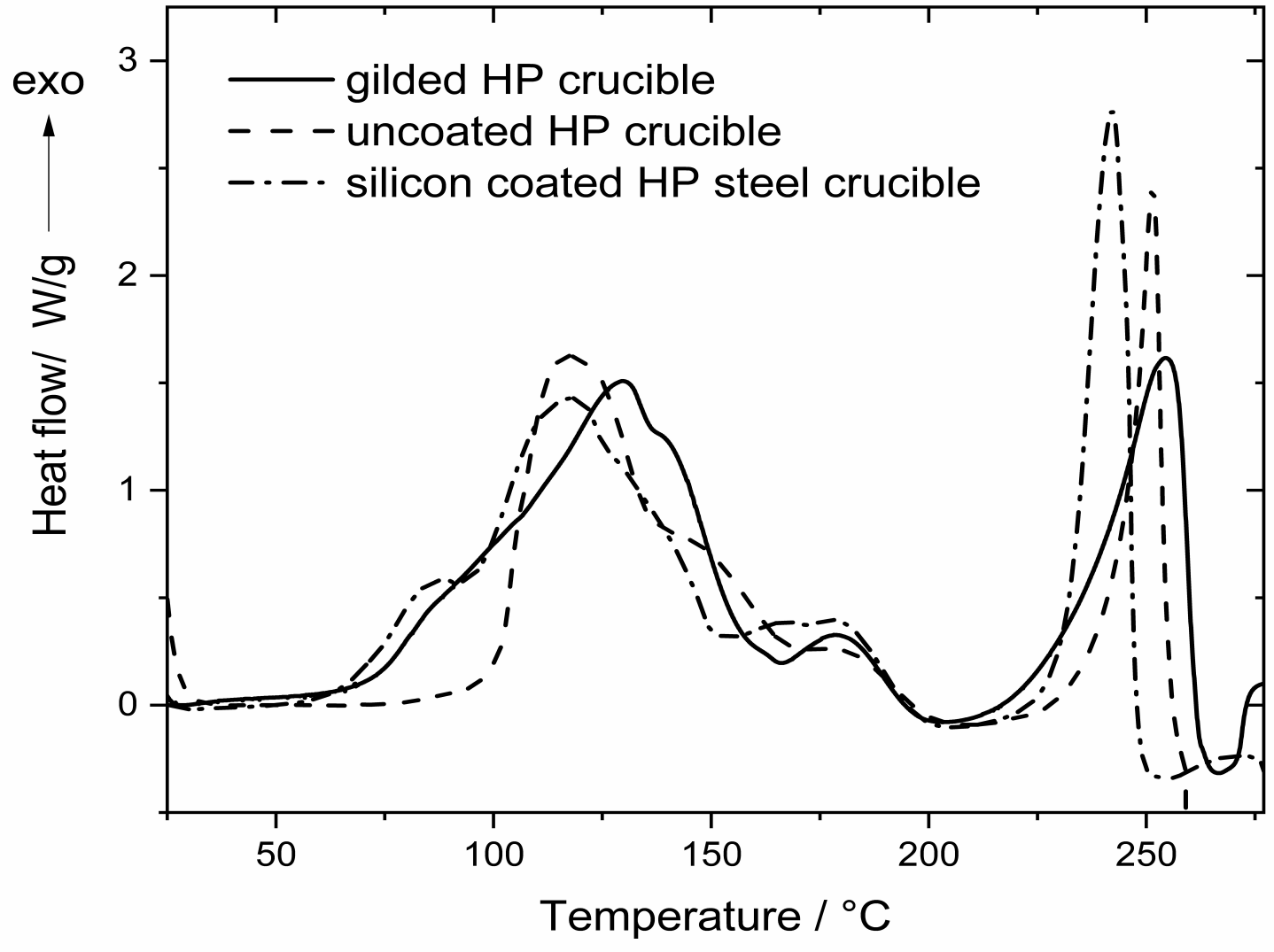
exo
Heat flow/ W/g
3
2
1
0
gilded HP crucible
uncoated HP crucible
silicon coated HP steel crucible
50
100
150
200
250
Temperature / °C

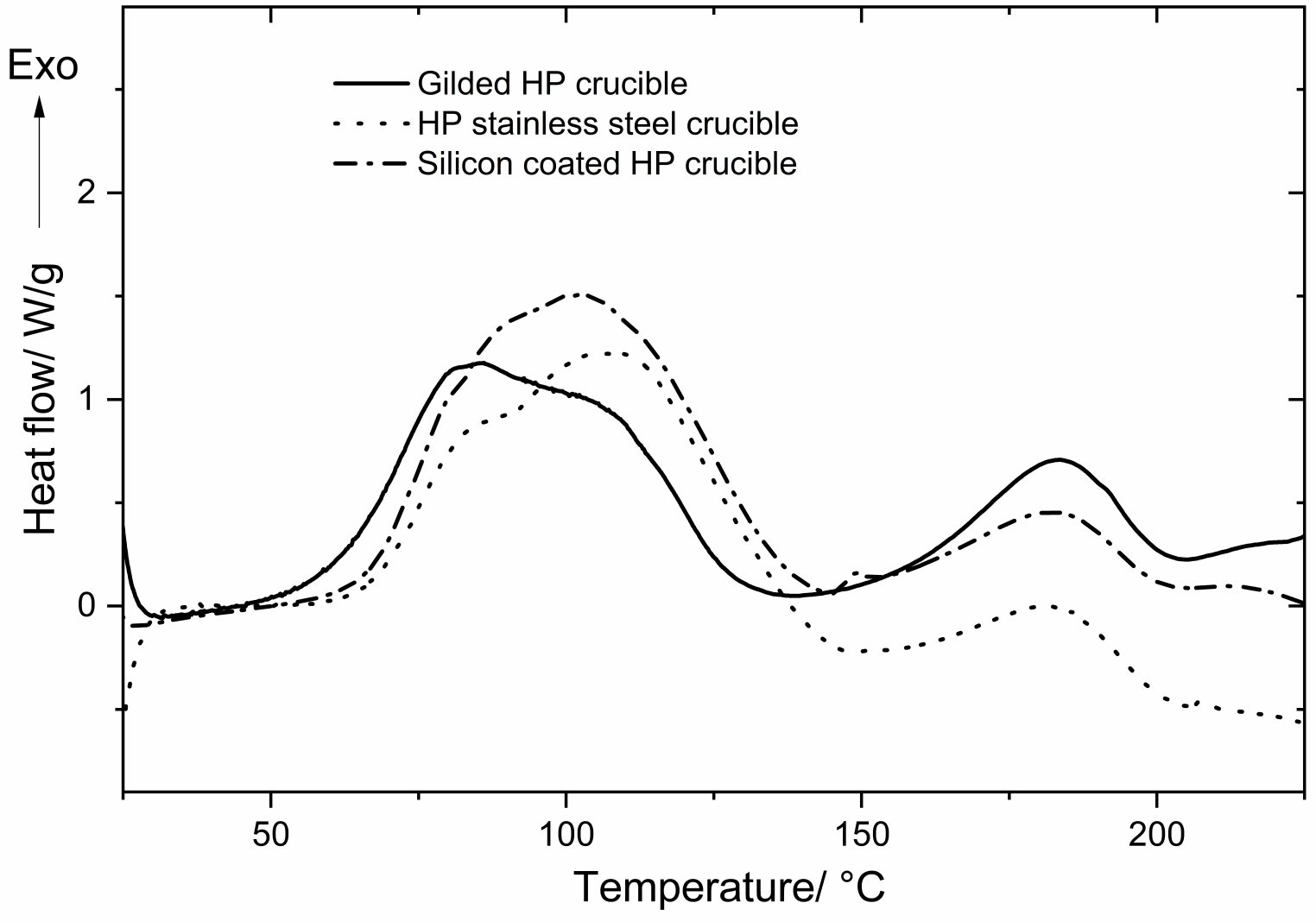
Exo
Heat flow/ W/g
2
1
0
Gilded HP crucible
HP stainless steel crucible
Silicon coated HP crucible
50
100
150
200
Temperature/ °C

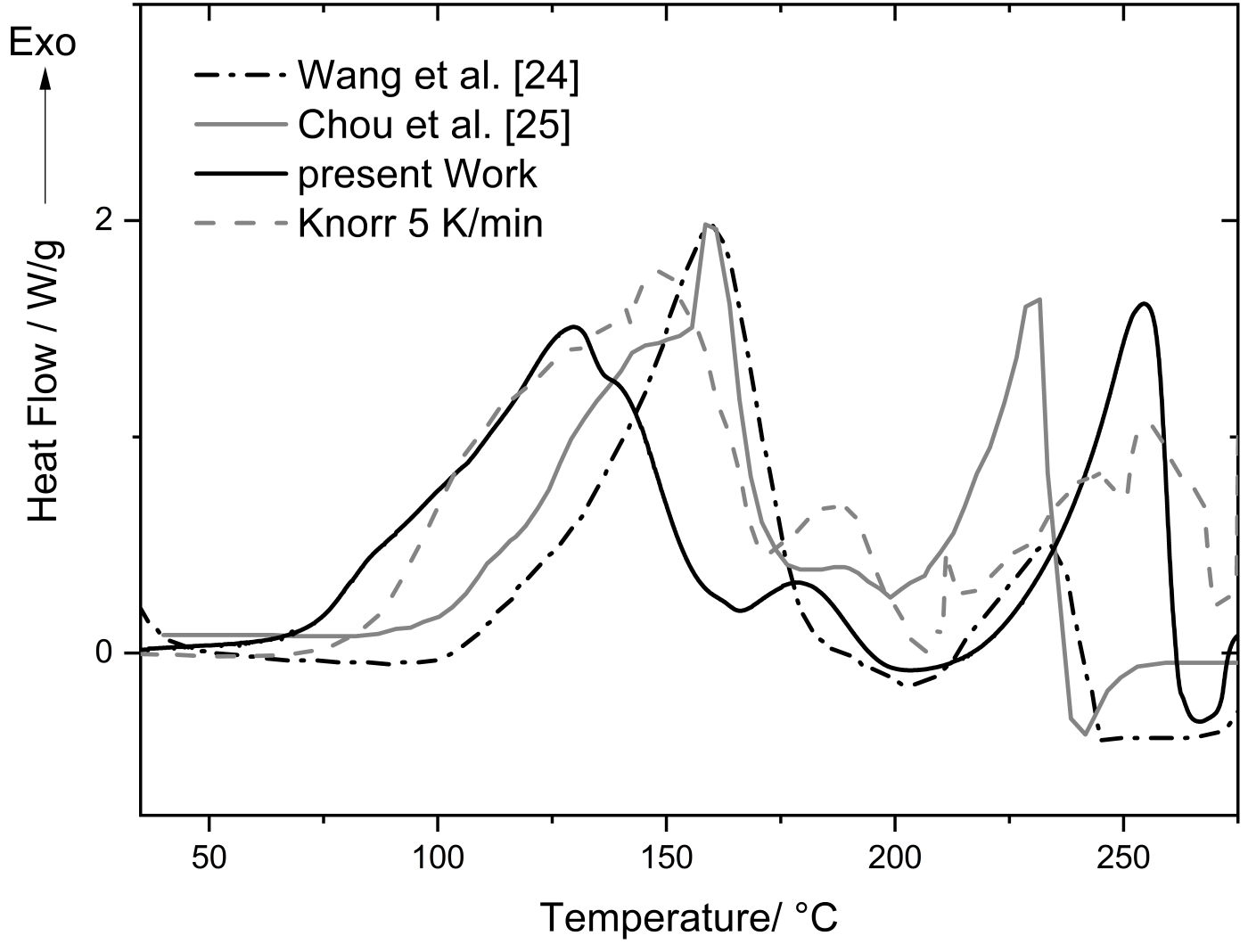
Exo
Heat Flow / W/g
2
0
Wang et al. [24]
Chou et al. [25]
present Work
Knorr 5 K/min
50
100
150
200
250
Temperature/ °C

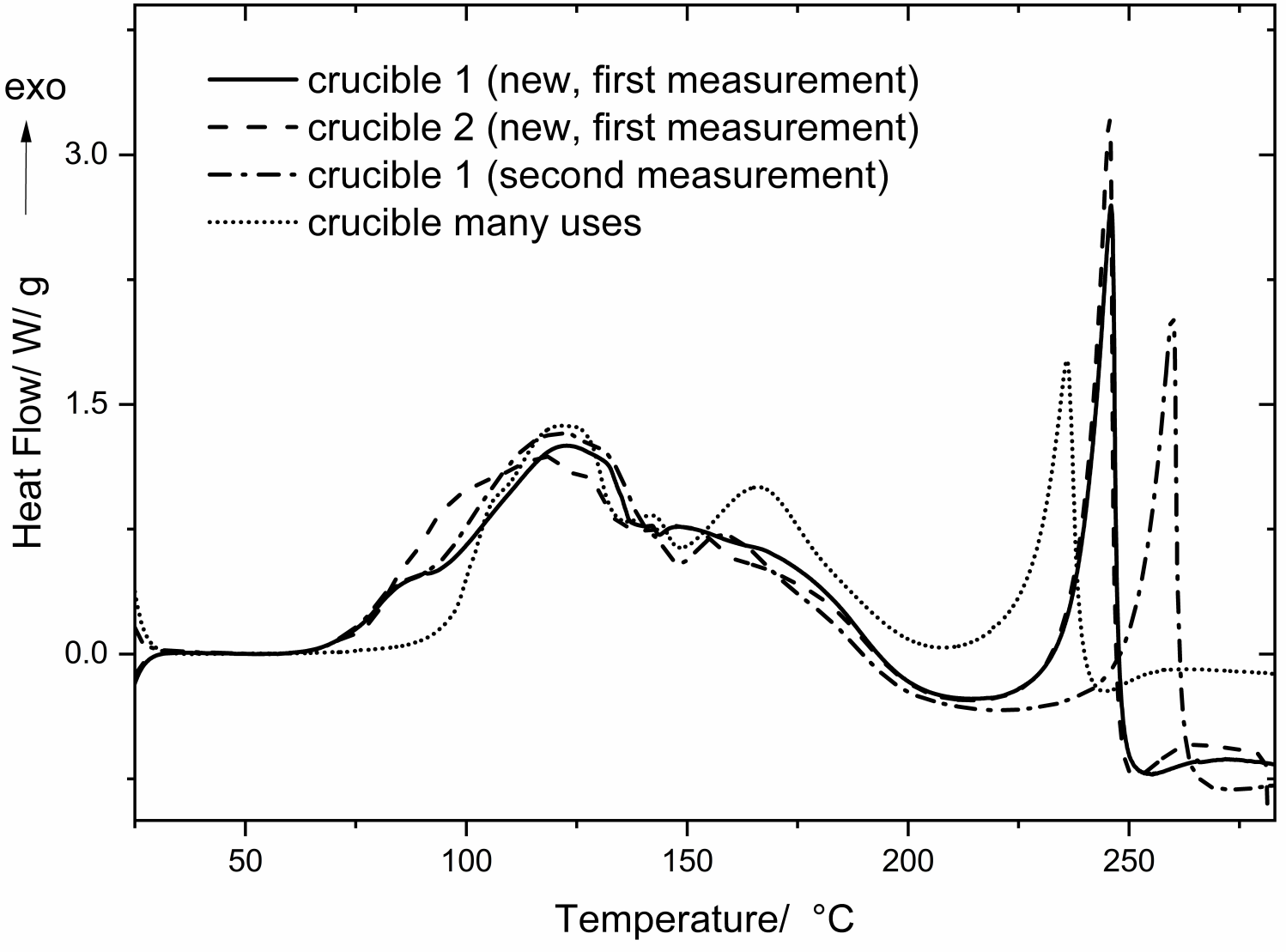
exo
Heat Flow/ W/ g
3.0
1.5
0.0
crucible 1 (new, first measurement)
crucible 2 (new, first measurement)
crucible 1 (second measurement)
crucible many uses
50
100
150
200
250
Temperature/ °C

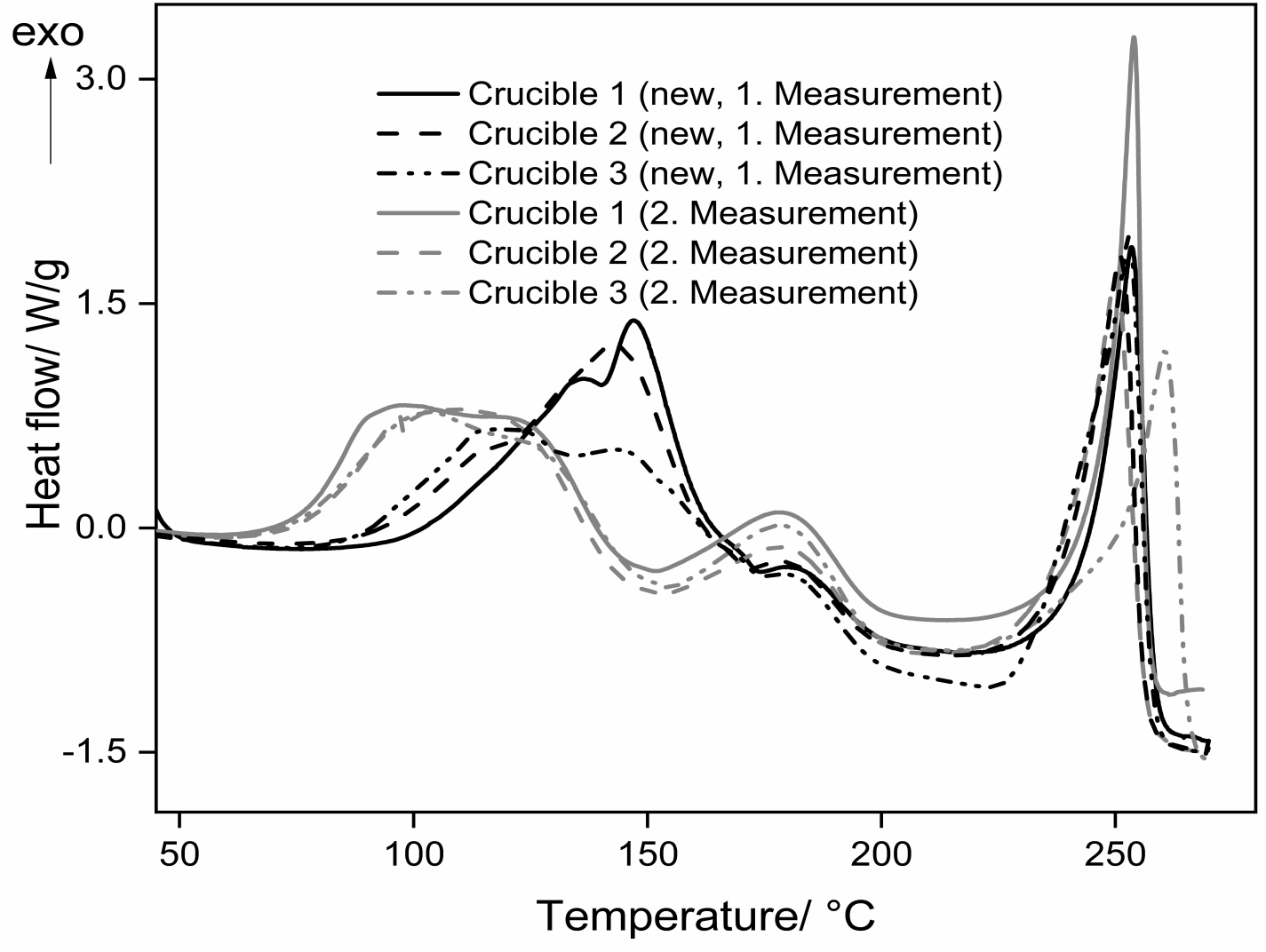
exo
3.0
1.5
0.0
-1.5
Heat flow/ W/g
Crucible 1 (new, 1. Measurement)
Crucible 2 (new, 1. Measurement)
Crucible 3 (new, 1. Measurement)
Crucible 1 (2. Measurement)
Crucible 2 (2. Measurement)
Crucible 3 (2. Measurement)
50
100
150
200
250
Temperature/ °C

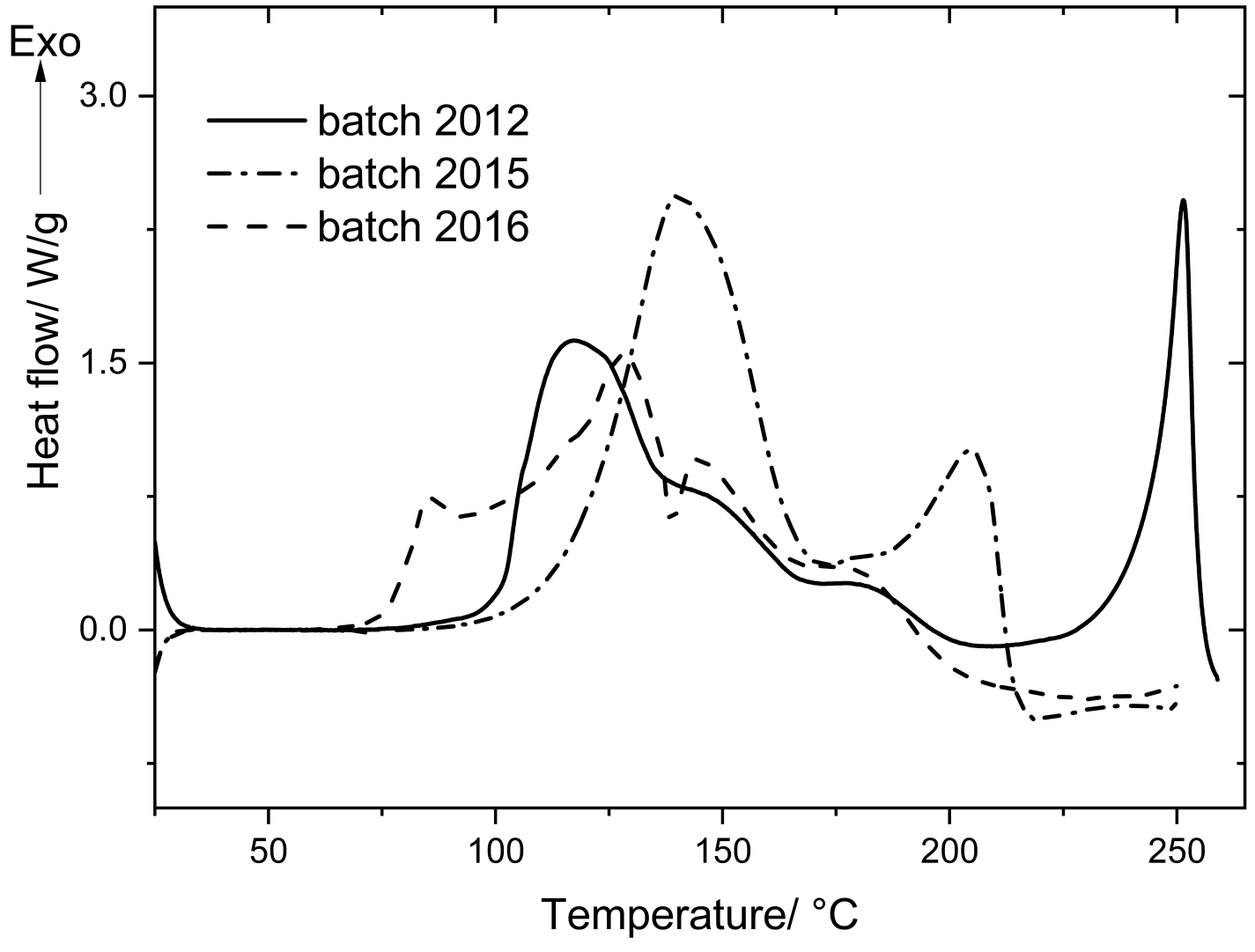
Exo
Heat flow/ W/g
3.0
1.5
0.0
batch 2012
batch 2015
batch 2016
50
100
150
200
250
Temperature/ °C

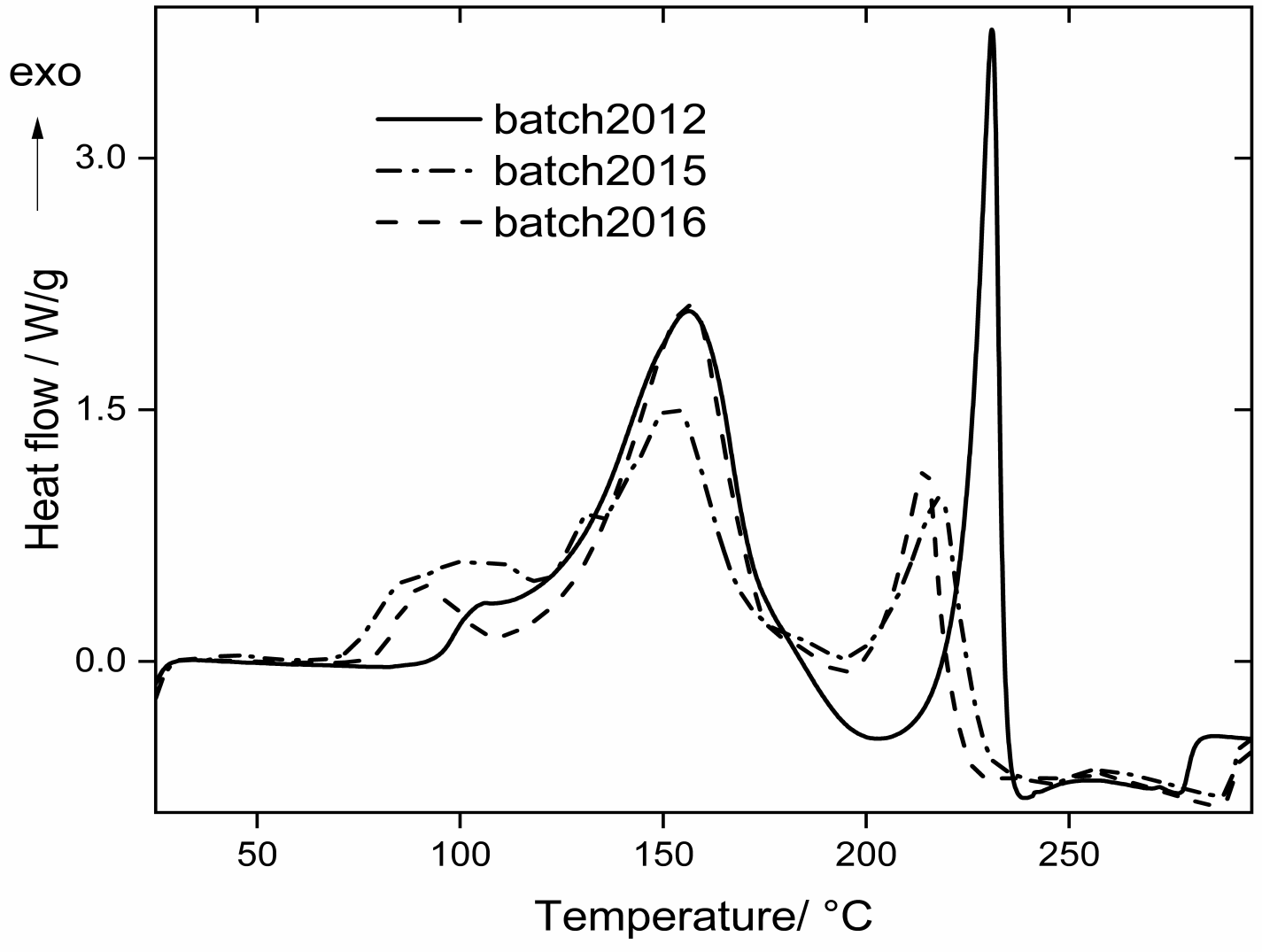
exo
Heat flow / W/g
3.0
1.5
0.0
batch2012
batch2015
batch2016
50
100
150
200
250
Temperature/ °C

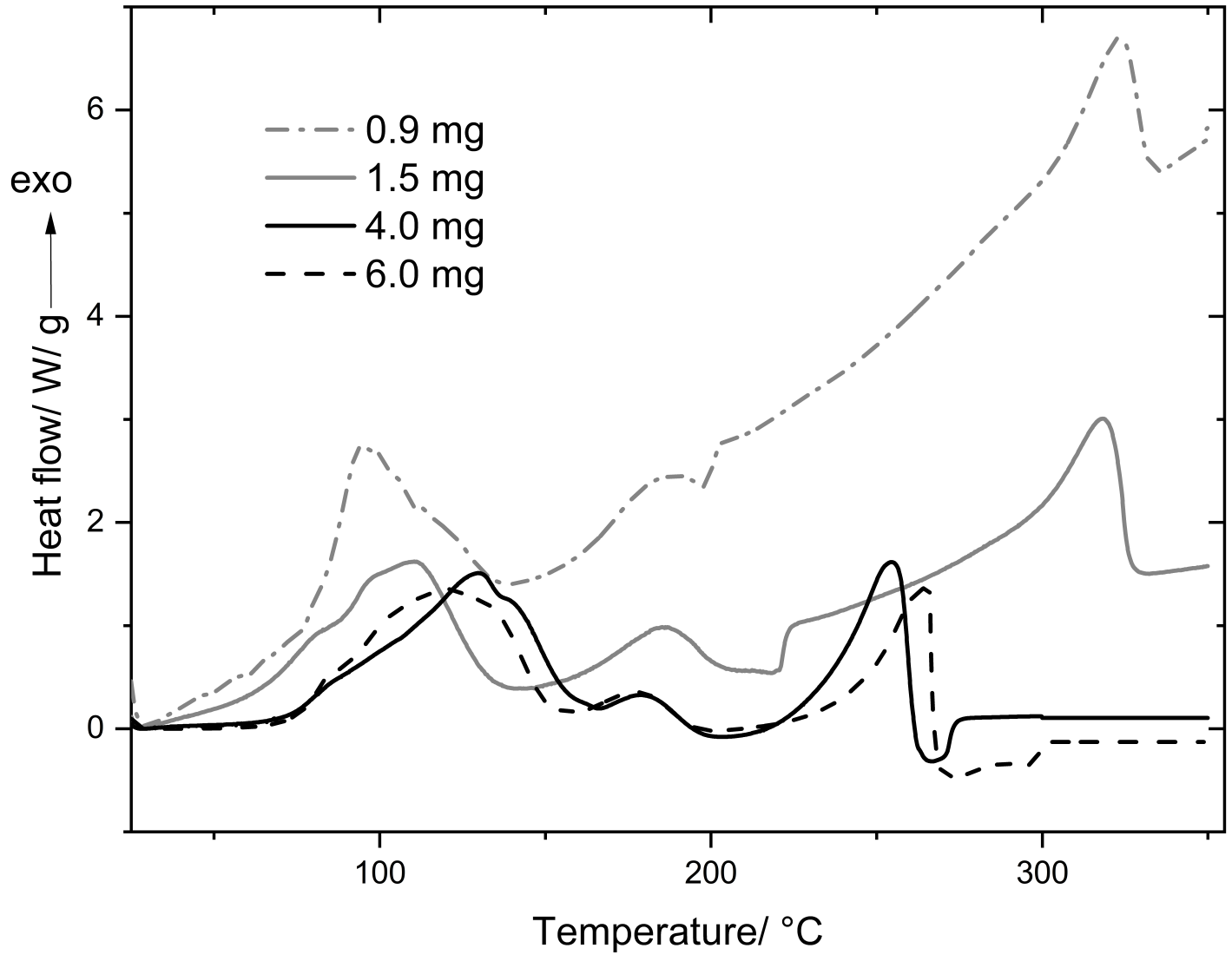
0.9 mg
1.5 mg
4.0 mg
6.0 mg
exo
Heat flow/ W/ g
6
4
2
0
100
200
300
Temperature/ °C

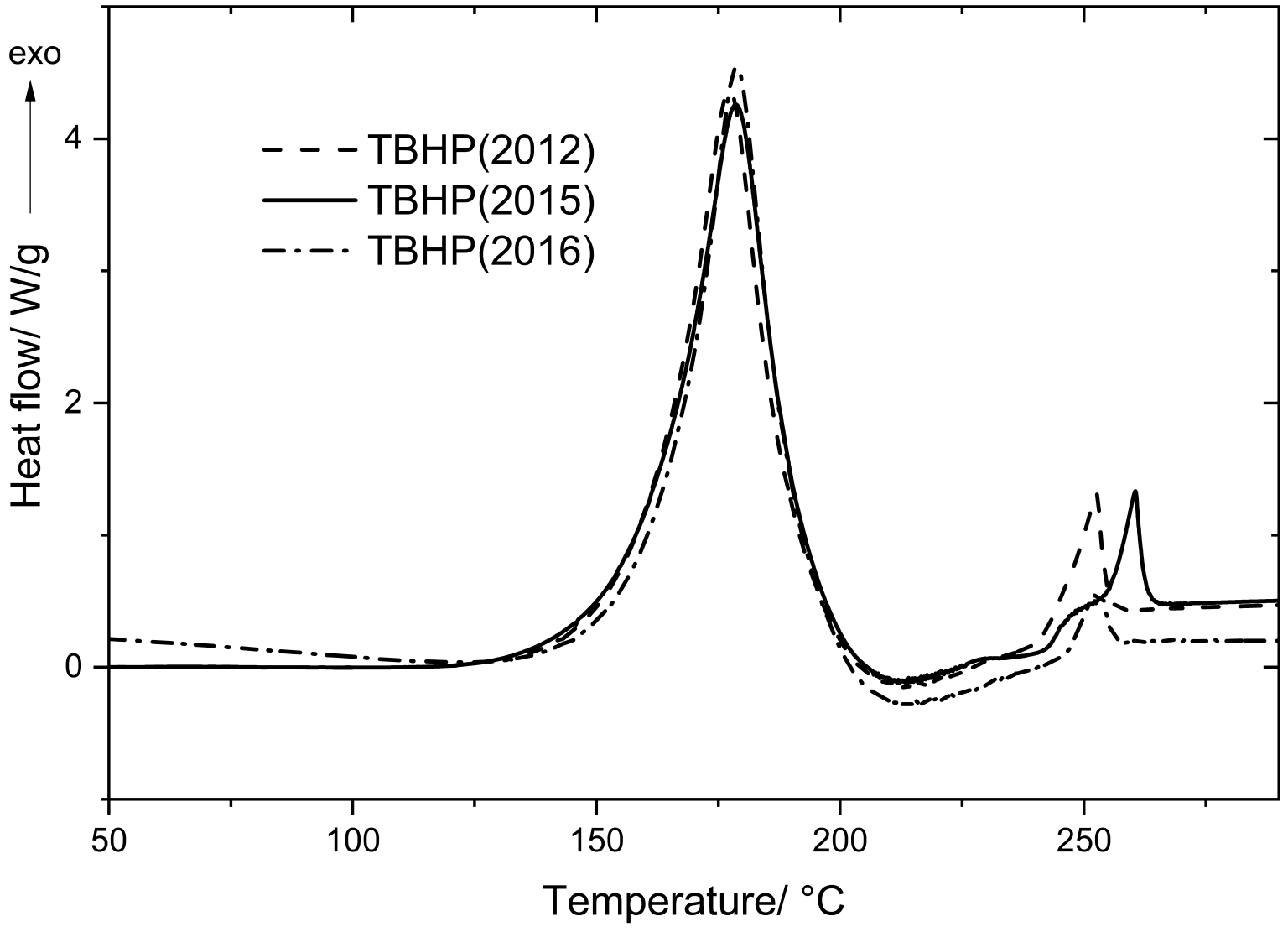
exo
Heat flow/ W/g
4
2
0
TBHP(2012)
TBHP(2015)
TBHP(2016)
50
100
150
200
250
Temperature/ °C

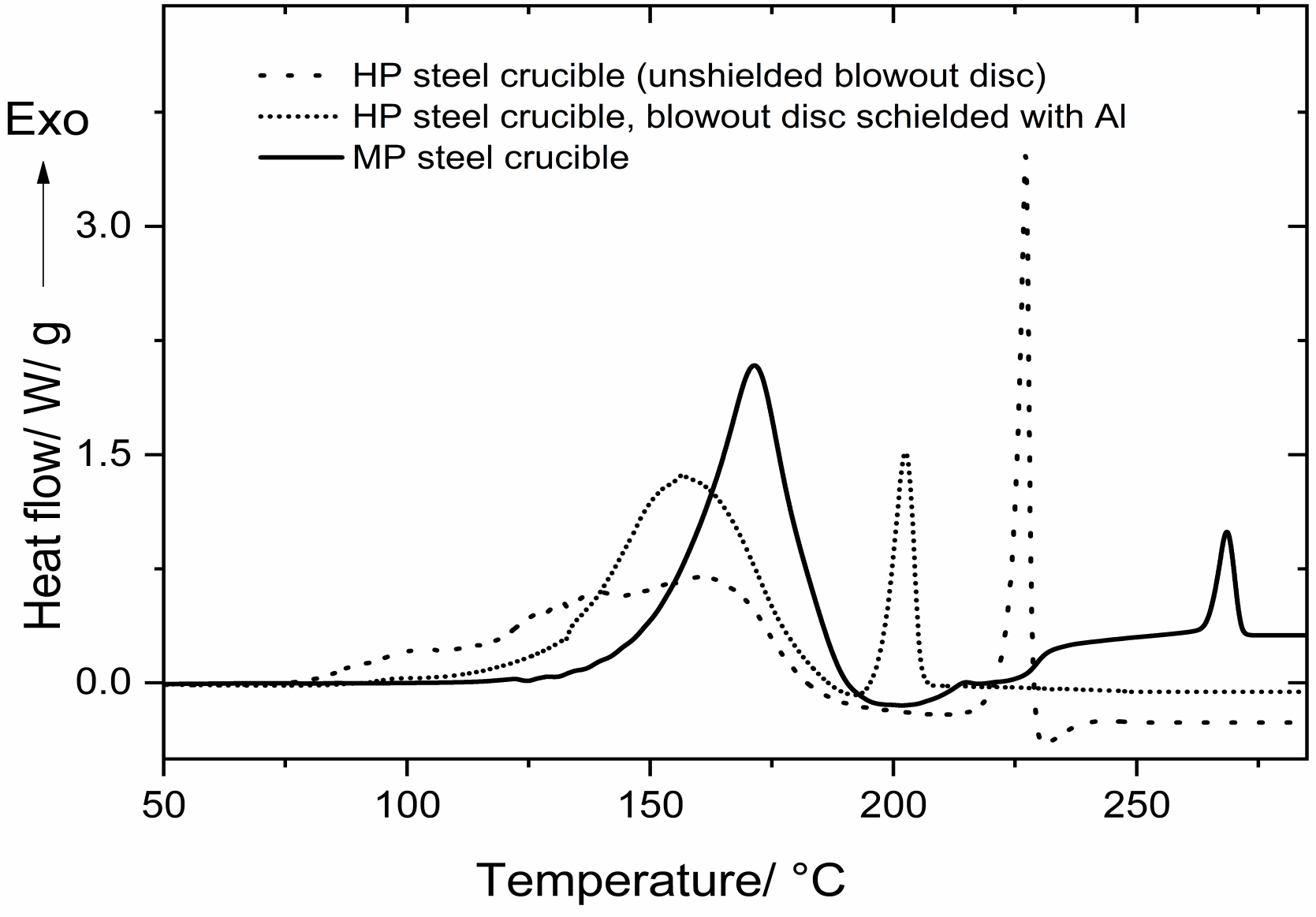
HP steel crucible (unshielded blowout disc)
HP steel crucible, blowout disc schielded with Al
MP steel crucible
Exo
Heat flow/ W/ g
3.0
1.5
0.0
50
100
150
200
250
Temperature/ °C

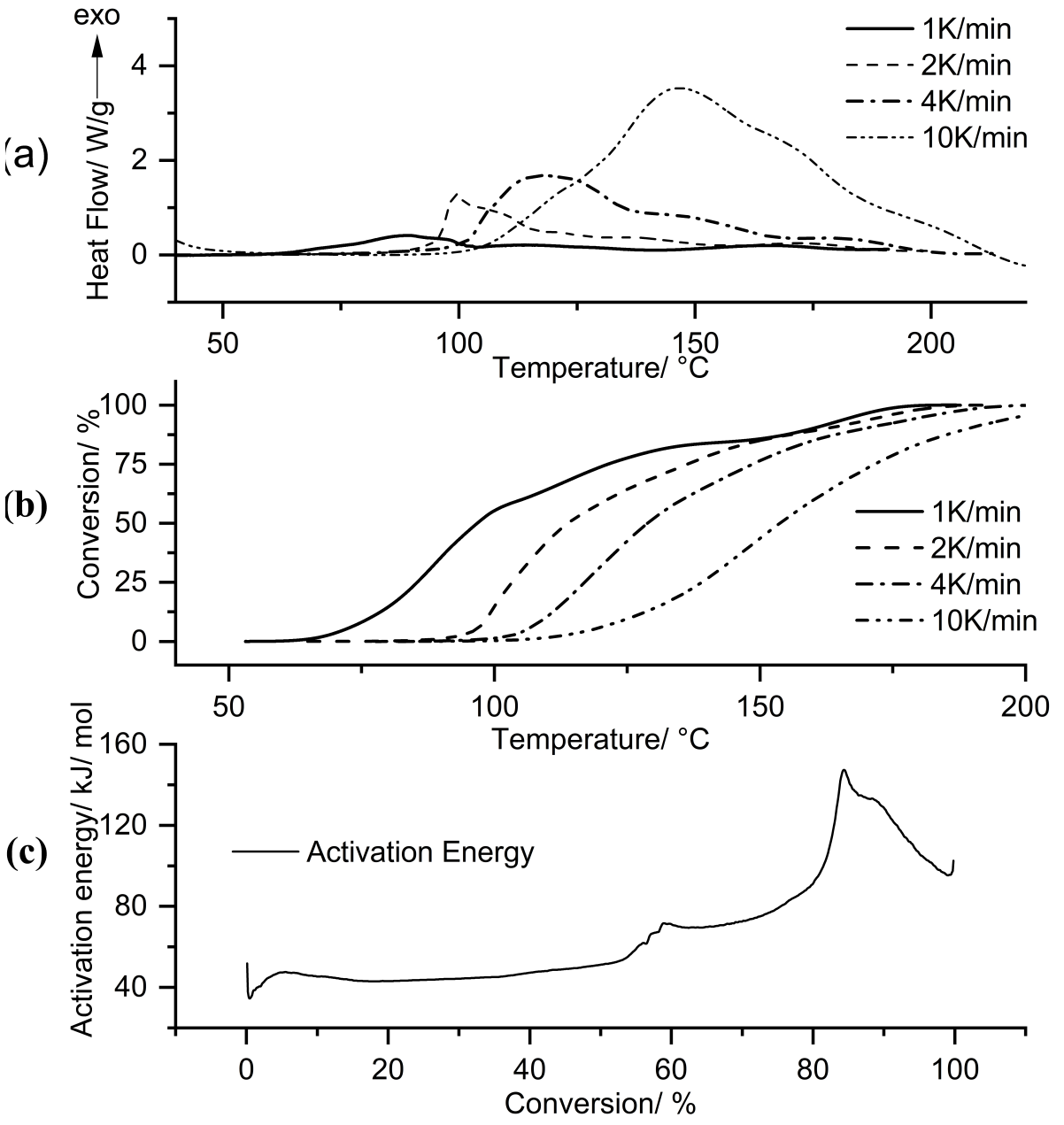
(a)
exo
Heat Flow/ W/g
4
2
0
1K/min
2K/min
4K/min
10K/min
50
100
150
200
Temperature/ °C
(b)
Conversion/ %
100
75
50
25
0
1K/min
2K/min
4K/min
10K/min
50
100
150
200
Temperature/ °C
(c)
Activation energy/ kJ/ mol
160
120
80
40
Activation Energy
0
20
40
60
80
100
Conversion/ %

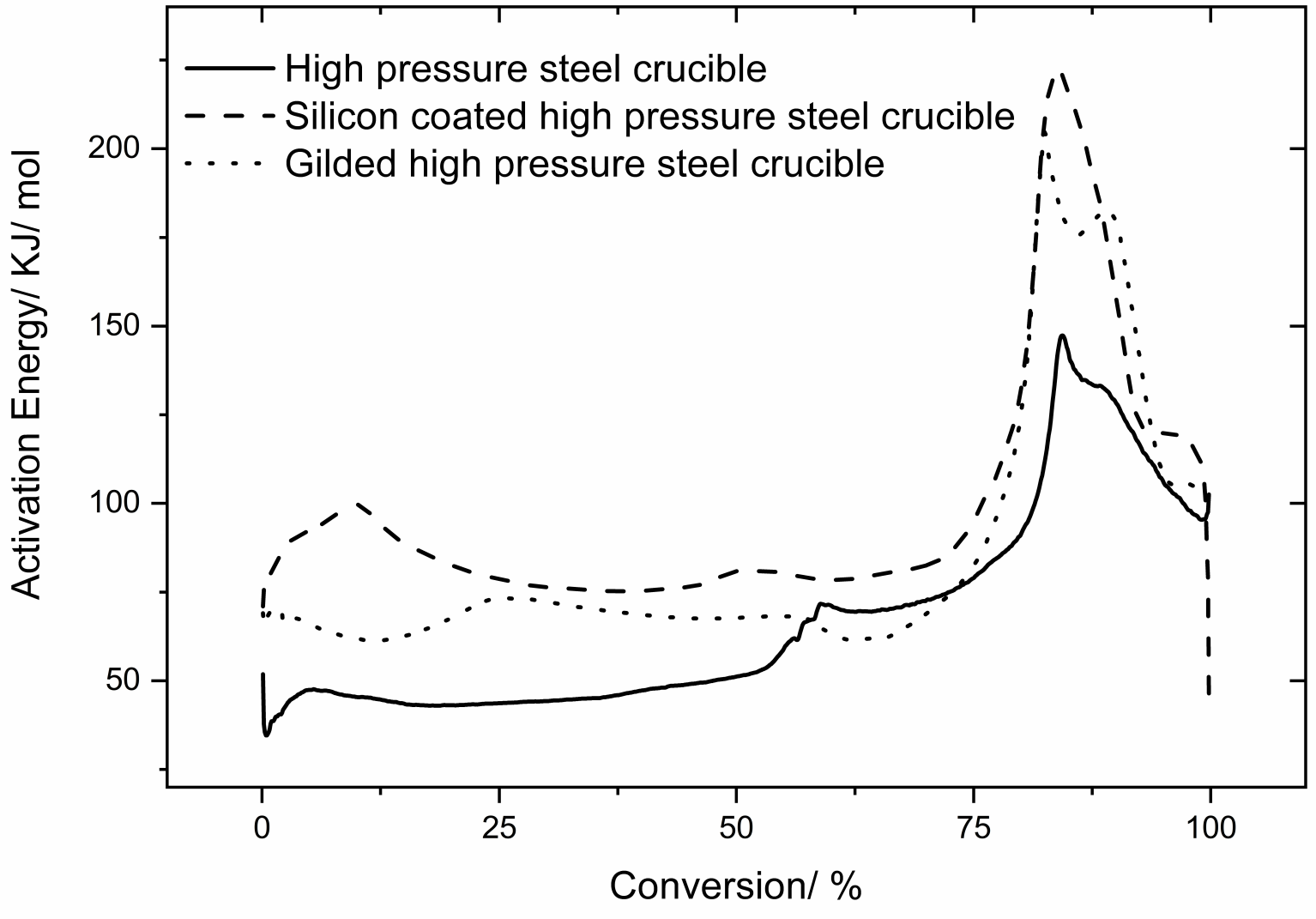
High pressure steel crucible
Silicon coated high pressure steel crucible
Gilded high pressure steel crucible
Activation Energy/ KJ/ mol
200
150
100
50
0
25
50
75
100
Conversion/ %

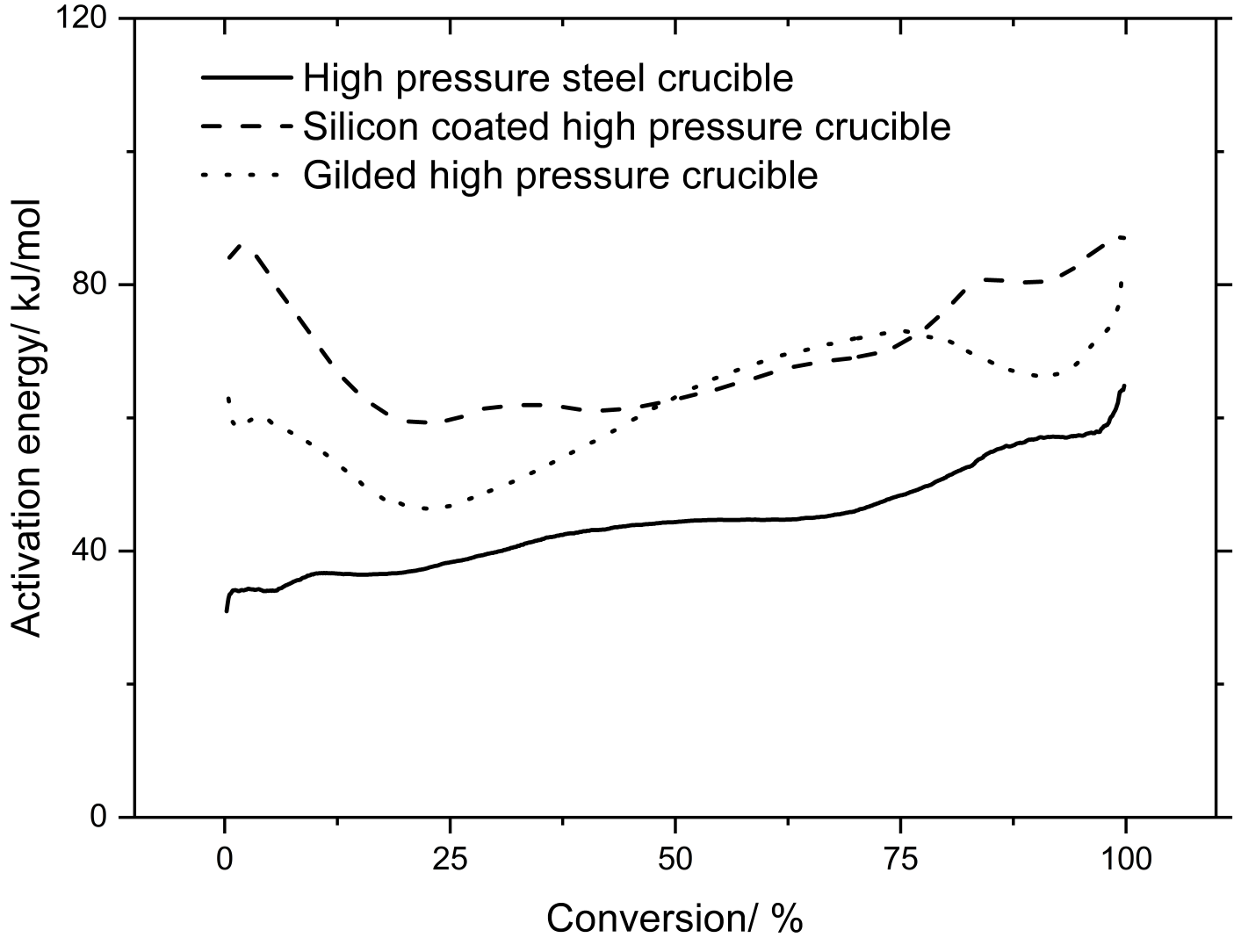
120
80
40
0
Activation energy/ kJ/mol
High pressure steel crucible
Silicon coated high pressure crucible
Gilded high pressure crucible
0
25
50
75
100
Conversion/ %

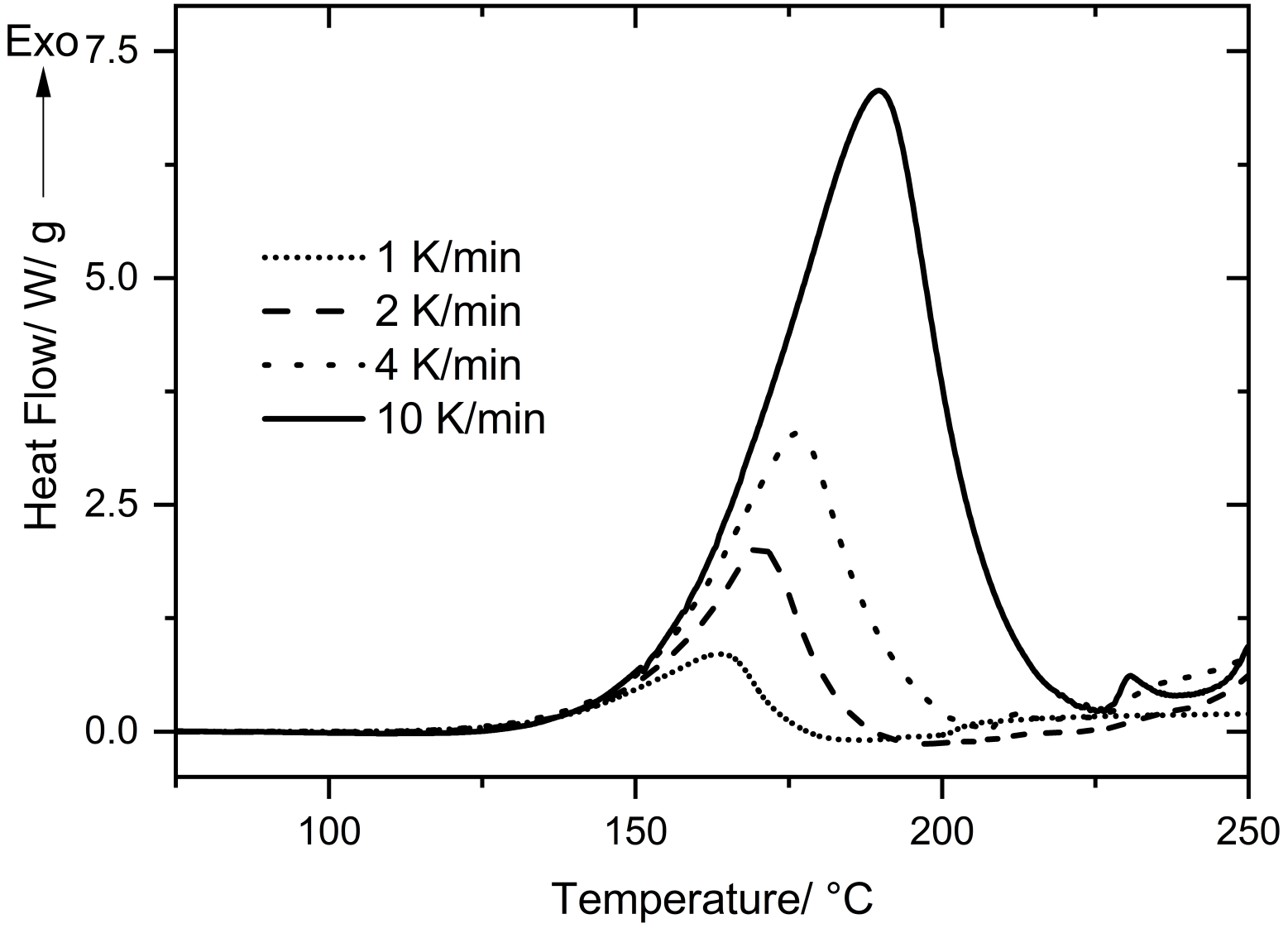
Exo
7.5
5.0
2.5
0.0
Heat Flow/ W/ g
1 K/min
2 K/min
4 K/min
10 K/min
100
150
200
250
Temperature/ °C

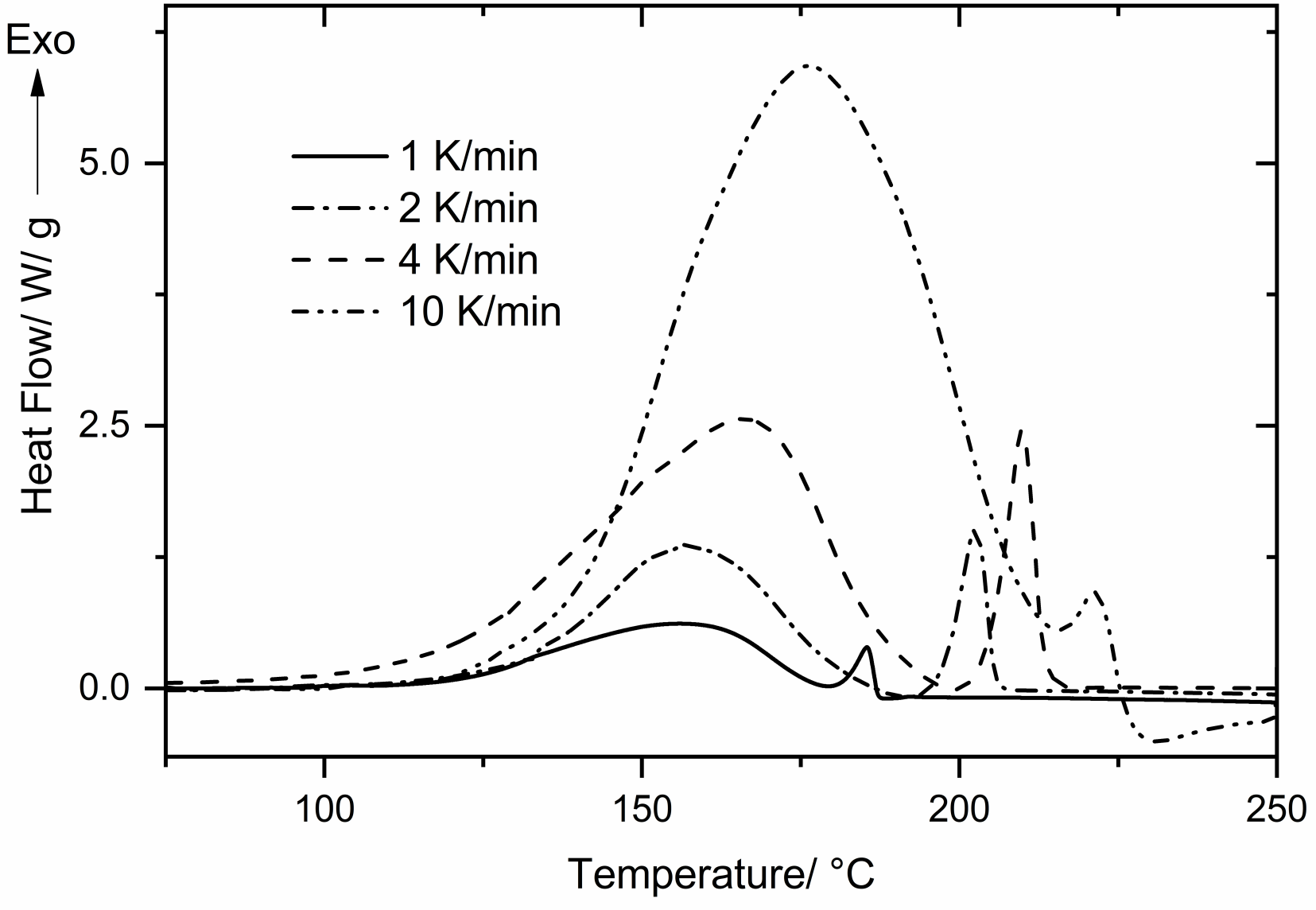
Exo
Heat Flow/ W/ g
5.0
2.5
0.0
1 K/min
2 K/min
4 K/min
10 K/min
100
150
200
250
Temperature/ °C

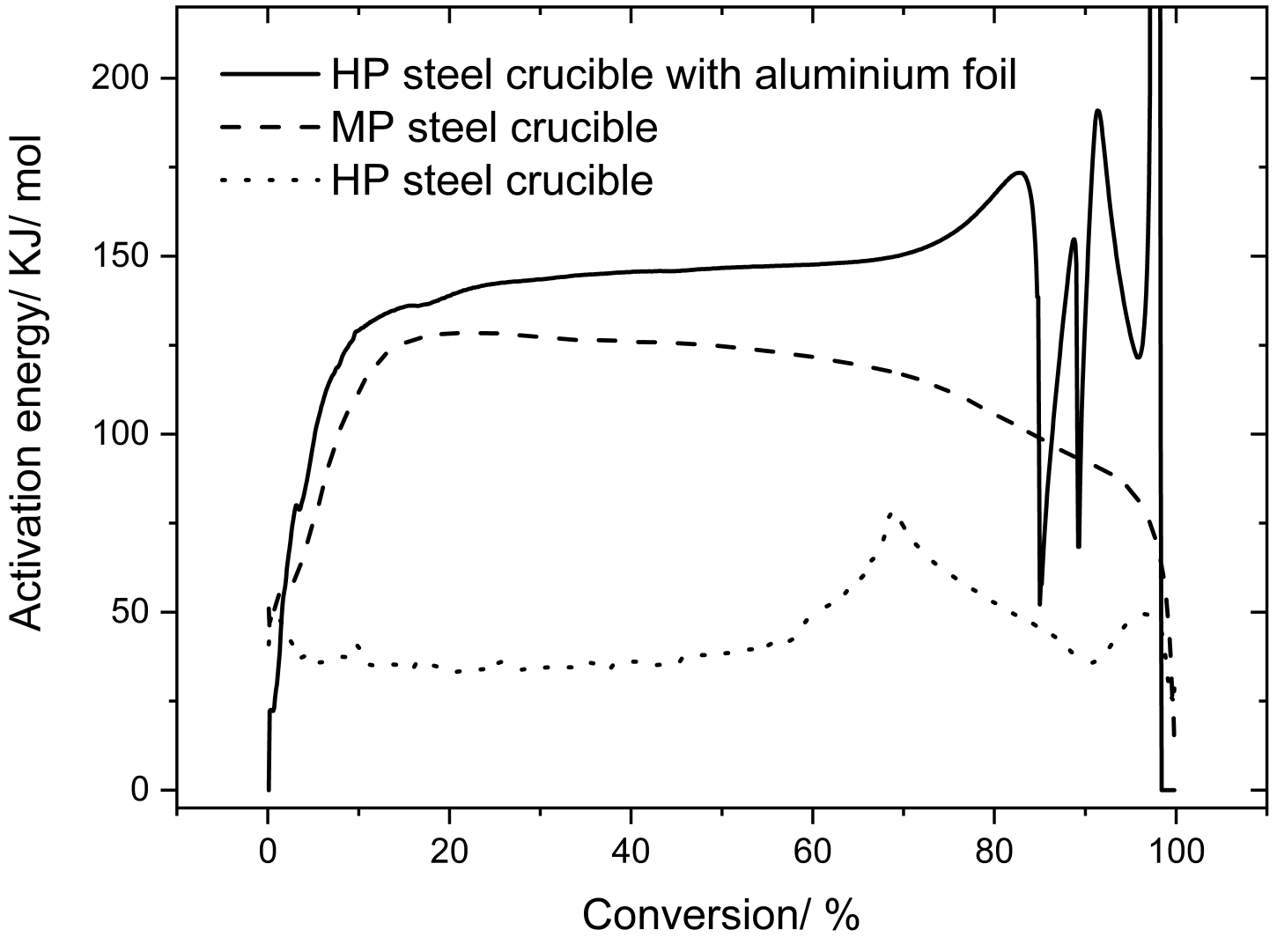
HP steel crucible with aluminium foil
MP steel crucible
HP steel crucible
Activation energy/ KJ/ mol
Conversion/ %
0
50
100
150
200
0
20
40
60
80
100

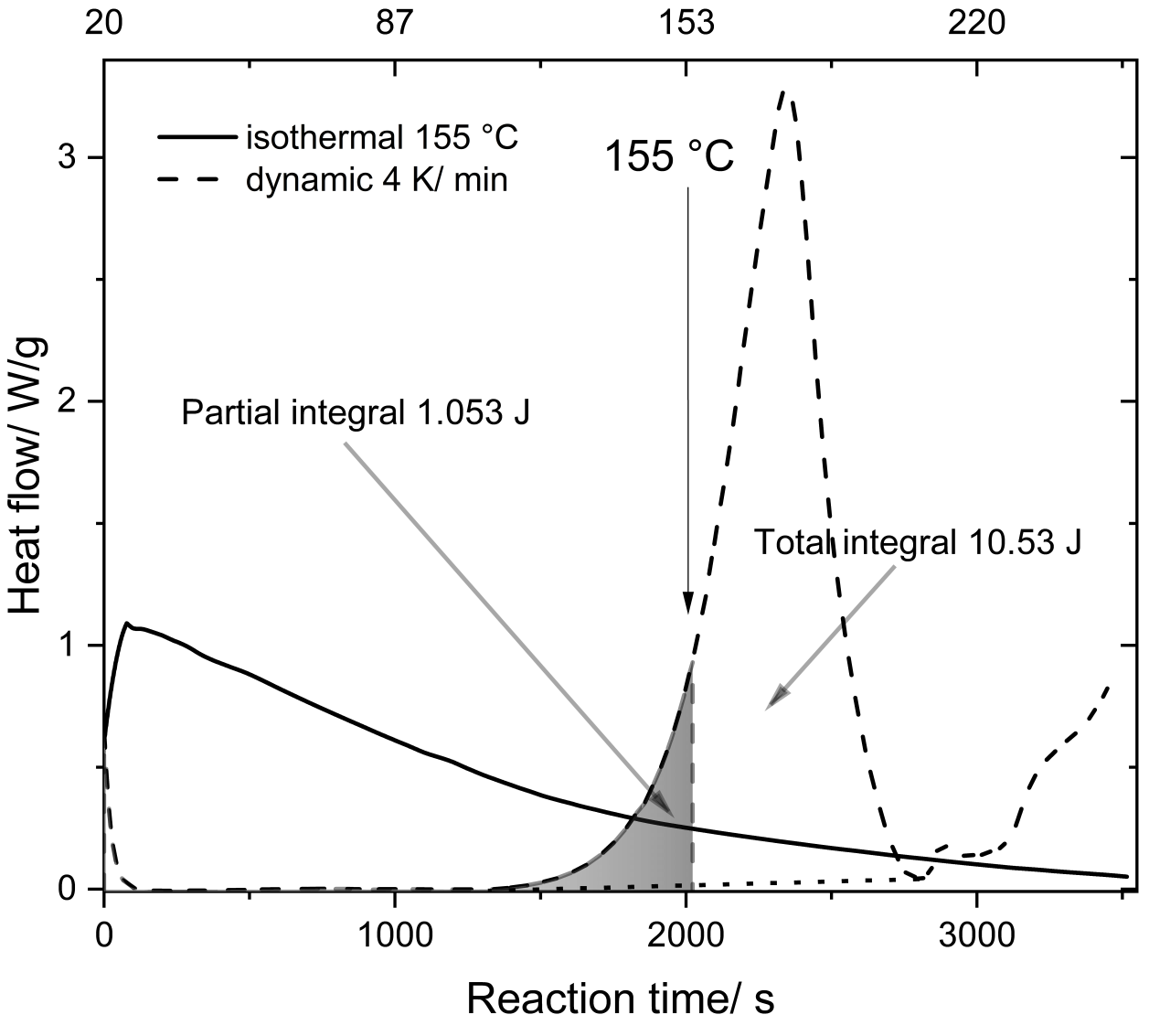
20
87
153
220
isothermal 155 °C
dynamic 4 K/ min
155 °C
Partial integral 1.053 J
Total integral 10.53 J
Heat flow/ W/g
0
1
2
3
0
1000
2000
3000
Reaction time/ s

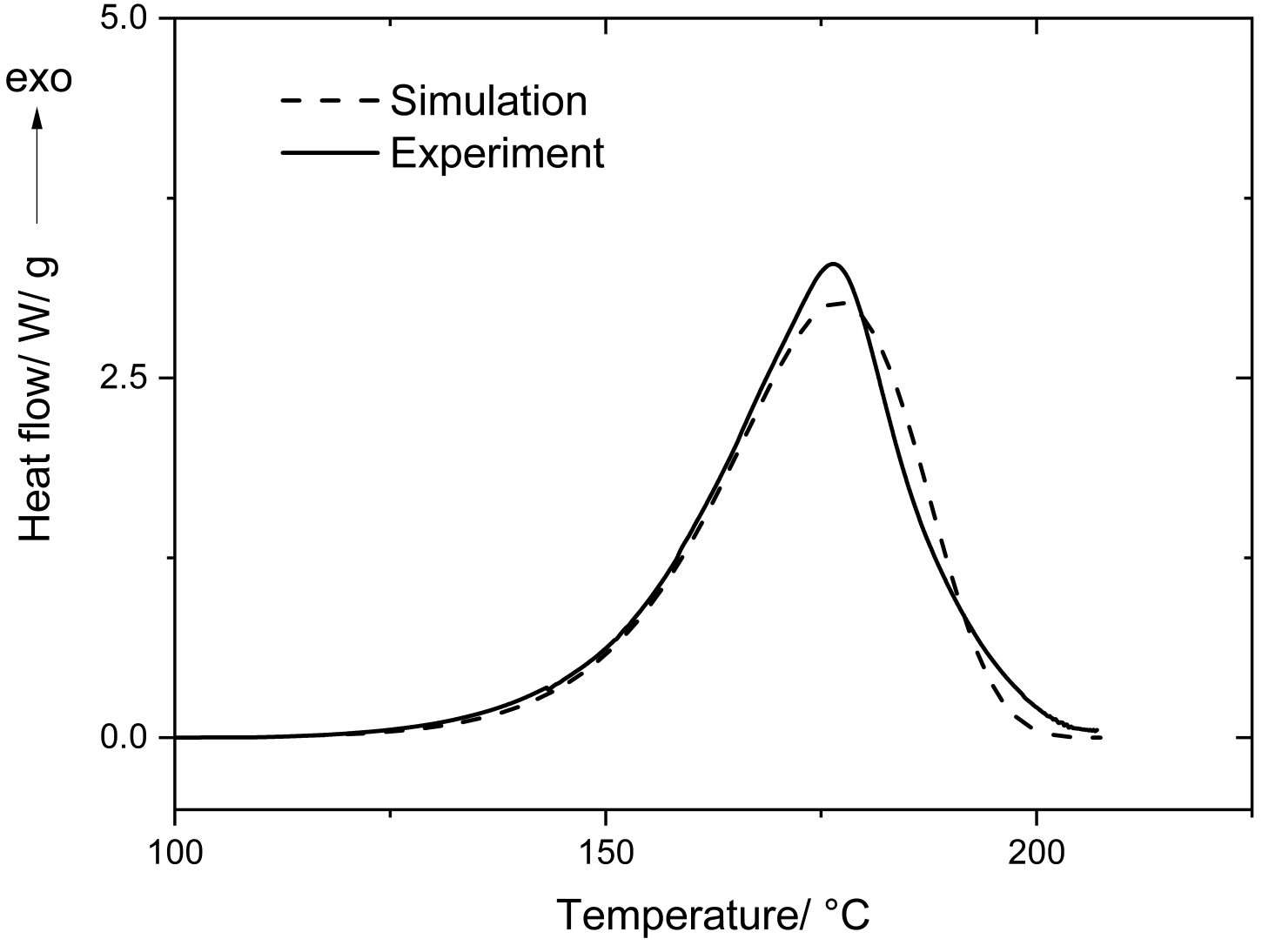
5.0
2.5
0.0
exo
Heat flow/ W/ g
Simulation
Experiment
100
150
200
Temperature/ °C

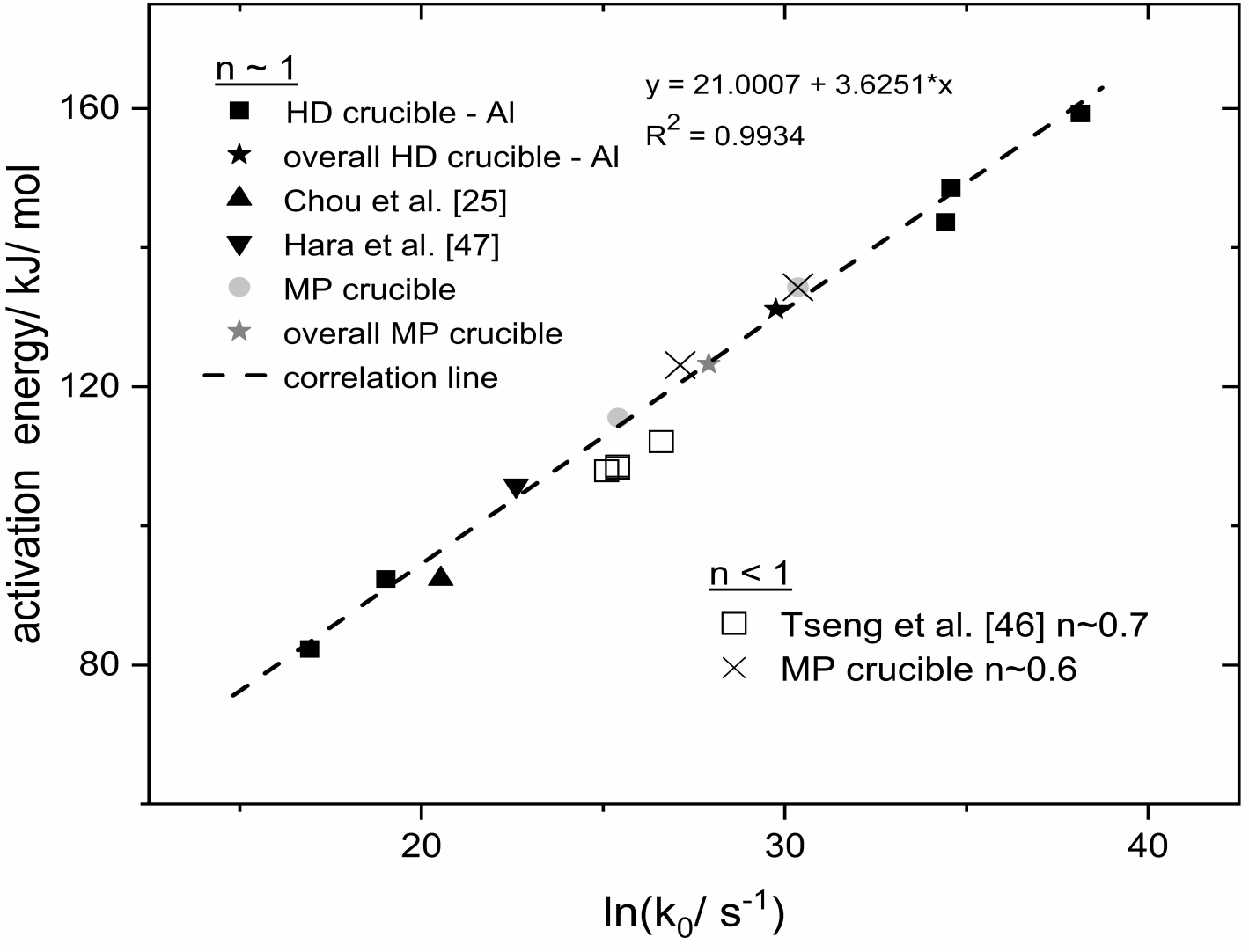
n ~ 1
HD crucible - Al
overall HD crucible - Al
Chou et al. [25]
Hara et al. [47]
MP crucible
overall MP crucible
correlation line
y = 21.0007 + 3.6251*x
R2 = 0.9934
n < 1
Tseng et al. [46] n~0.7
MP crucible n~0.6
activation energy/ kJ/ mol
160
120
80
20
30
40
ln(k0/ s-1)